A REGIONAL EVALUATION OF MANNING'S ROUGHNESS ESTIMATES IN STREAMS OF SOUTH-CENTRAL TEXAS

THESIS

Presented to the Graduate Council of
Southwest Texas State University
in Partial Fulfillment of
the Requirements

For the Degree

Master of Applied Geography

By

Mindy M. Conyers, B.S.

San Marcos, Texas
August 2003

ACKNOWLEDGEMENTS

I want to thank Dr. Mark Fonstad for providing countless hours of support and encouragement and for turning the simple wish of doing a thesis involving fieldwork into a reality. His guidance and vast knowledge gave my academic life a distinct direction towards the goal of completing this program. I would also like to thank Dr. Richard Earl for giving much needed help and advice in keeping both my thesis and my life on track. Dr. David Butler deserves thanks as well for balancing constructive criticism and humor in his efforts to get this study finished. The endless patience and guidance given by these three professors afforded me the opportunity to spend time doing two of my favorite things- driving around the beautiful Texas hill country and splashing around in rivers.

Thanks are also due to my parents, Jim and Sharon Conyers, for giving me the courage and strength required to survive this thesis and graduate school. As well they provided humor and much needed assistance in the field on multiple occasions with smiles on their faces all the while. My sister, Jamie Conyers, deserves thanks for helping me complete the bulk of the fieldwork necessary for this thesis. Her comic relief and skillful data recording kept the process of traipsing around below forbidding overpasses and braving blustery weather enjoyable enough to make me forget that my hands were frozen. My aunt, Brenda Pruitt, and cousin, Eli Pruitt, also provided much appreciated field assistance. Even though the weather thwarted our efforts to collect much data, the experience was still a joy. Without all of this help from different family members the process of data collection might have seemed arduous rather than so enjoyable.

LIST OF FIGURES

CHAPTER I

INTRODUCTION

The Manning equation is perhaps the most commonly used hydraulic technique for estimating river velocity. The equation combines measurements of channel geometry and slope with an estimate of resistance to flow (Manning's *n* or roughness) to estimate stream velocity. Stream discharge is calculated by multiplying this estimated velocity by the channel's cross-sectional area (Dingman and Sharma 1997, 14; Graf and Randall 1997, 6; Knighton 1998, 101; Li and Zhan 2001, 153; Manning 1891; Marcus et al. 1992, 228; Tinkler 1997, 147).

This research answers the following questions: Can channel roughness be analyzed at the regional scale to reveal geographic patterns across south-central Texas? Which commonly used velocity estimation equation produces the most accurate results for streams in this region? Can data collected for this research produce new equations that are optimized for accuracy within this region?

This research presents a new method for calculating channel roughness based on the Manning equation, field data, and historically collected stream measurements. Substantial error can be introduced when estimating discharge based on the Manning equation resulting from poor estimates of flow resistance. In addition, spatial distributions of hydraulic roughness are often complex and may confound attempts to represent river processes over large areas.

Accurate estimates of stream discharge in the south-central Texas region are critical to water resource management and land use management strategies. Stream discharge data can be used for flood hazard prediction, irrigation management, and habitat conservation. Discharge records are often unavailable, however, at remote stream sections where gages are not present. Hence, stream discharge is often calculated using rapid estimation techniques based on stream morphology (Dingman and Sharma 1997, 14; Marcus et al. 1992, 228; Tinkler 1997, 147).

This research fits well within the perspective of geography because its focus is the physical phenomena that shape the local environment. Geographers express "the changing patterns of places in words, maps, and geographics, explain how these patterns come to be, and unravel their meaning" (Bednarz, Boehm, and Downs 1994). This research specifically investigates patterns of channel roughness, evaluates methods to predict this roughness, and provides a guide for estimating river velocity in south-central Texas. Understanding how local processes affect not just the physical environment but also the people living there is key to viewing the world through the eyes of a geographer.

CHAPTER II

BACKGROUND

Theoretical Framework

The Manning equation is a widely applied regression equation developed during the late 1800s by engineer Robert Manning. His work involved the collection of hundreds of measurements in irrigation canals in order to develop a method for estimating stream flow (Dingman and Sharma 1997, 14; Graf and Randall 1997, 6; Manning 1891, 162). The Manning equation is

$$v = \frac{R^{0.67} S^{0.5}}{n} \tag{1}$$

where v is velocity in meters per second, S is the slope, and n is the roughness coefficient. R is the hydraulic radius in meters, which is equal to the cross-sectional area divided by the wetted perimeter. The exponent of R is an average of the range of exponents (0.65 to 0.84) obtained for various channel shapes and roughnesses. Velocity and the cross-sectional area are multiplied to estimate discharge (Graf and Randall 1997, 6; Manning 1891; Marcus et al. 1992, 228).

The roughness coefficient, n, cannot be measured directly. It must be estimated either using techniques requiring channel measurements or through those techniques requiring only visual estimates (Dingman and Sharma 1997, 15; Graf and Randall 1996, 6; Marcus et al. 1992, 228). Over the years, five models have been commonly used to generate values for Manning's *n* (Table 1).

Use of *n* is complicated by the fact that resistance to flow can vary with discharge, flow depth, particle size, sediment load, turbulence, vegetation, obstructions, sinuosity, and interactions between these factors. A further complication arises from the adjustments in bedform, and hence channel roughness, that accompany changes in flow regime. Also the Manning equation was developed for streams of one steady, uniform flow. A steady flow is one in which velocity is constant with time. Uniform flow exists when the gravitational and frictional components of the channel are in balance. In a channel with uniform flow velocity is constant with position. Completely accurate use of this equation is thus limited to such a stream. However in natural channels with erodable boundaries the resistance problem is much more involved (Dingman and Sharma 1997, 15; Graf and Randall 1997, 45; Knighton 1998, 101; Marcus et al. 1992, 228).

Channel roughness directly affects flow resistance, which in turn determines how much energy the stream has available for sediment transport and channel erosion (Graf and Randall 1997, 74). Total flow resistance actually consists of several components. These include boundary resistance, channel resistance, and free surface resistance. Boundary resistance results from the friction created when water passes over the channel bed material. Channel resistance is a function of the irregularity of the bank. Waves and hydraulic jumps within the channel result in free form resistance The measure of roughness, *n*, used in the Manning equation incorporates all these forms of energy loss into one value (Bathurst 1993; Knighton 1998, 101; Tinkler 1997, 151).

Table 1. Techniques for estimating roughness (Marcus et al 1992)

Source	**Equation or Method**
Barnes 1967	USGS Picture Book
Bathurst 1985	$n = \dfrac{0.3194R^{0\ 167}}{4.0 + 5.62\log(R/d_{84})}$
Cowan 1956	$n = (n_0 + n_1 + n_2 + n_3 + n_4)m_5$
Jarrett 1984	$n = 0.32S^{0\ 38}R^{-0\ 16}$
Limerinos 1970	$n = \dfrac{0.1129R^{0\ 167}}{1.16 + 2.0\log(R/d_{84})}$

For the purposes of this research, discharge refers to the amount of water passing through a channel at a given time, calculated by multiplying stream flow velocity and cross-sectional area (Knighton 1998, 378; Wahl et al. 1995, 14). Particle size refers to the size of the clasts that are transported and deposited along a streambed. Turbulence is the degree of deviation of water parcels from parallel laminar flow (Knighton 1998, 382). Obstructions may include things such as large clasts, gravel bars, or man-made features. Sinuosity refers to the degree of meandering of a stream (Knighton 1998, 382). Slope is the ratio of change in elevation to the length of the longest mapped channel (Graf and Randall 1997, 75; Slade et al. 1995). Stage is defined as the height of the water surface above some reference elevation (Wahl et al. 1995).

Field Measurement Techniques

A number of techniques developed for making estimates of *n* require the collection of field measurements for various channel characteristics. This research evaluates the local accuracy of those equations developed by Limerinos (1970), Jarrett (1984), and Bathurst (1985), which incorporate data that must be collected in the field (Marcus et al. 1992, 228).

The impact of particle size on roughness can be so great in some channels that techniques were developed to estimate roughness essentially based on sediment size. Both the Limerinos equation and Bathurst's equation are based on reaches where sediment is the primary source of roughness (Bathurst 1985; Limerinos 1970, 5).

Limerinos (1970)
$$n = \frac{0.1129R^{0.167}}{1.16 + 2.0\log(R/d_{84})} \quad (2)$$

Bathurst (1985) $$n = \frac{0.3194R^{0\,167}}{4.0 + 5.62\log(R/d_{84})} \tag{3}$$

Again R is the hydraulic radius in meters and d_{84} represents the 84th percentile of pebble size across the channel. Both equations provide reasonable estimates of roughness in relatively low gradient streams with sediment of gravel size or smaller (Bathurst 1985; Limerinos 1970, 17; Richards 1982, 66). In steeper mountain streams where particle sizes are as great as the flow depth, however, these equations are often inaccurate and underestimate Manning's n. These underestimates may occur because the equations largely ignore sources of resistance such as changes in channel shape, bedform, sinuosity, hydraulic jumps, vegetation, obstructions, and sediment load which are common in mountain settings (Jarrett 1984, 1522; Marcus et al. 1992, 236).

A second technique requiring field measurements is Jarrett's equation

$$n = 0.32S^{0\,38}R^{-0\,16} \tag{4}$$

which relates roughness to hydraulic variables. In mountain streams, Jarrett (1984) used multiple regression to develop an equation relating roughness to slope and hydraulic radius. In this situation, slope provides an effective measure of flow resistance because as slope increases so do bed particle size, wake turbulence, and energy lost in hydraulic jumps (Jarrett 1984, 1522; Marcus et al. 1992, 229). In a study conducted by Marcus et al. (1992) in the Juneau Icefields of Alaska, Jarrett's equation provided the most accurate results for estimating n when compared to ten other techniques (Marcus et al. 1992, 236). Other studies also concluded that Jarrett's equation provides the most reliable roughness estimates in general (Dingman and Sharma 1997, 31; Graf and Randall 1997, 74).

Visual Estimate Techniques

In addition to the previous techniques, which require collection of field data, several other approaches approximate channel roughness solely from visual estimates (Dingman and Sharma 1997, 15; Graf and Randall 1996, 6; Marcus et al. 1992, 228). In one such approach, deemed the USGS picture book approach, the researcher compares pictures of streams with known roughness coefficients to a channel in the field. Based on the range of photographs, the scientist then chooses an appropriate n value for the stream (Barnes 1967, 4). Photographic roughness estimates intended for a given depth of flow proved to be inappropriate in the mountains of Alaska based on the Marcus et al. (1992) study. These photographic guides are generally intended for one depth of flow and do not provide good roughness estimates for other discharges. Still the photographic approach is inexpensive and simple to conduct in the field (Graf and Randall 1997, 74; Marcus et al. 1992, 228).

A second technique for estimating n based on visual estimates was developed by Cowan (1956, 473) and incorporates many of the factors that may affect roughness. This component approach breaks the roughness estimate into six factors: sediment size (n_0); degree of surface irregularity (n_1); variation of channel cross-section (n_2); effect of obstructions (n_3); vegetation (n_4); and degree of meandering (m_5). The total roughness, n, is calculated from:

$$n = (n_0 + n_1 + n_2 + n_3 + n_4)m_5 \tag{5}$$

All six roughness factors can be determined by visual observations and require no field measurements, although n_0 may be estimated from other studies which relate roughness to sediment size and flow depth (Cowan 1956, 473; Marcus et al. 1992, 229). In streams with sediments of gravel size and larger, for instance, Jarrett (1984) used Benson and Dalrymple's (1967, 21) roughness coefficients for bed material to estimate n_0 (Jarrett 1984, 1523). Also, Limerinos' (1970) *n* values based on sediment size and hydraulic radius are approximately equivalent to n_0 (Limerinos 1970, 15). Marcus et al. (1992) found in their Alaska study that Cowan's technique drastically underestimated roughness in the mountain setting (Marcus et al. 1992, 237). Both the USGS picture book method and Cowan's approach are subject to great error resulting from differences in the experience and expertise of the user.

Summation

Previous research comparing the accuracy of the different estimating techniques is inconclusive. Bray (1979, 47) found that Limerinos' (1970) equation was more accurate than Cowan's (1956) technique in gravel bed streams in Alberta, Canada. He noted, however, that the Cowan method was almost as accurate as the Limerinos equation and had the advantage of not requiring field measurements of particle size (Bray 1979, 49). Bray's work was representative of relatively low gradient streams and was conducted during high flows where ratios of hydraulic radius to particle size were high (Marcus et al. 1992, 231). The overall conclusion of the Marcus et al. (1992) study showed that in small mountain streams, Jarrett's equation provided the most accurate estimate of roughness. The remaining techniques tested underestimated *n*, sometimes by an order of magnitude (Marcus et al. 1992, 236). Little research has been done to determine the accuracy of these techniques for estimating roughness in the streams of the Texas Hill Country. This research tests five techniques- Limerinos', Bathurst's, Jarrett's, the USGS picture book method, and Cowan's- for estimating roughness in streams in south-central Texas.

CHAPTER III

STUDY AREA

The study area for this research is the region in south-central Texas referred to as the Edwards Plateau (Figure 1). The Edwards Plateau is a unique natural region in Texas bordered to the north by the High Plains, Rolling Plains, and Oak Woods and Prairies, to the east by the Blackland Prairie, the south by the South Texas Brush Country, and to the west by the Trans Pecos region. Located almost entirely within the Edwards Plateau is the Llano Uplift (TPWD 2002).

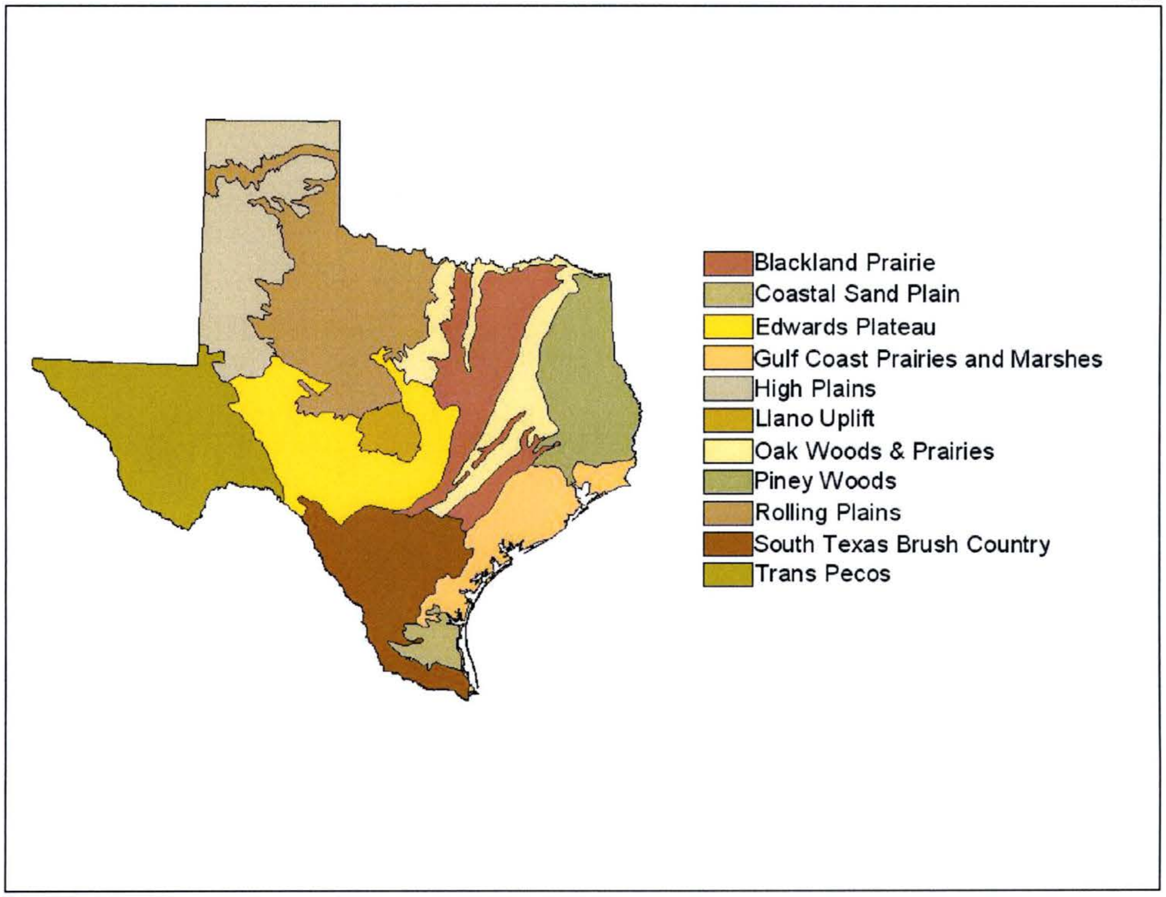

Fig. 1. Natural Regions of Texas (TPWD 2002)

The elevation of the plateau decreases gradually eastward (from about 1200m to roughly 400m) until it drops abruptly at the edge of the dissected limestone wall that is the Balcones Escarpment (Swanson 1995, 27). The Edwards Plateau lies within the Texas Hill Country and Balcones Canyonlands landform districts of the Edwards Plateau landform section of the Great Plains landform province (Fenneman 1931; Fenneman 1938).

Most notably the geological processes that occurred on the Edwards Plateau influence almost every aspect of the local environment on the plateau. During the Precambrian Era, two continental plates collided at what is now the Balcones Escarpment, which resulted in the formation of large granite batholiths (the Llano Uplift natural region). Later in the Mesozoic Era (Cretaceous Period), shallow oceans covered central Texas depositing mud and the shells of crustaceans, which over time formed into thick layers of limestone. Significant uplifting occurred during the Cenozoic Era in the form of branching normal faults along the Balcones Fault Zone. As the Edwards Plateau rose, local streams cut deep canyons into the limestone surface (Figure 2). Differential erosion of resistant limestone and softer marl layers of the area resulted in the stair-stepped topography typical of the Edwards Plateau today (Petersen and Tuason 1995a, 12; Petersen and Tuason 1995b, 21; Swanson 1995, 28).

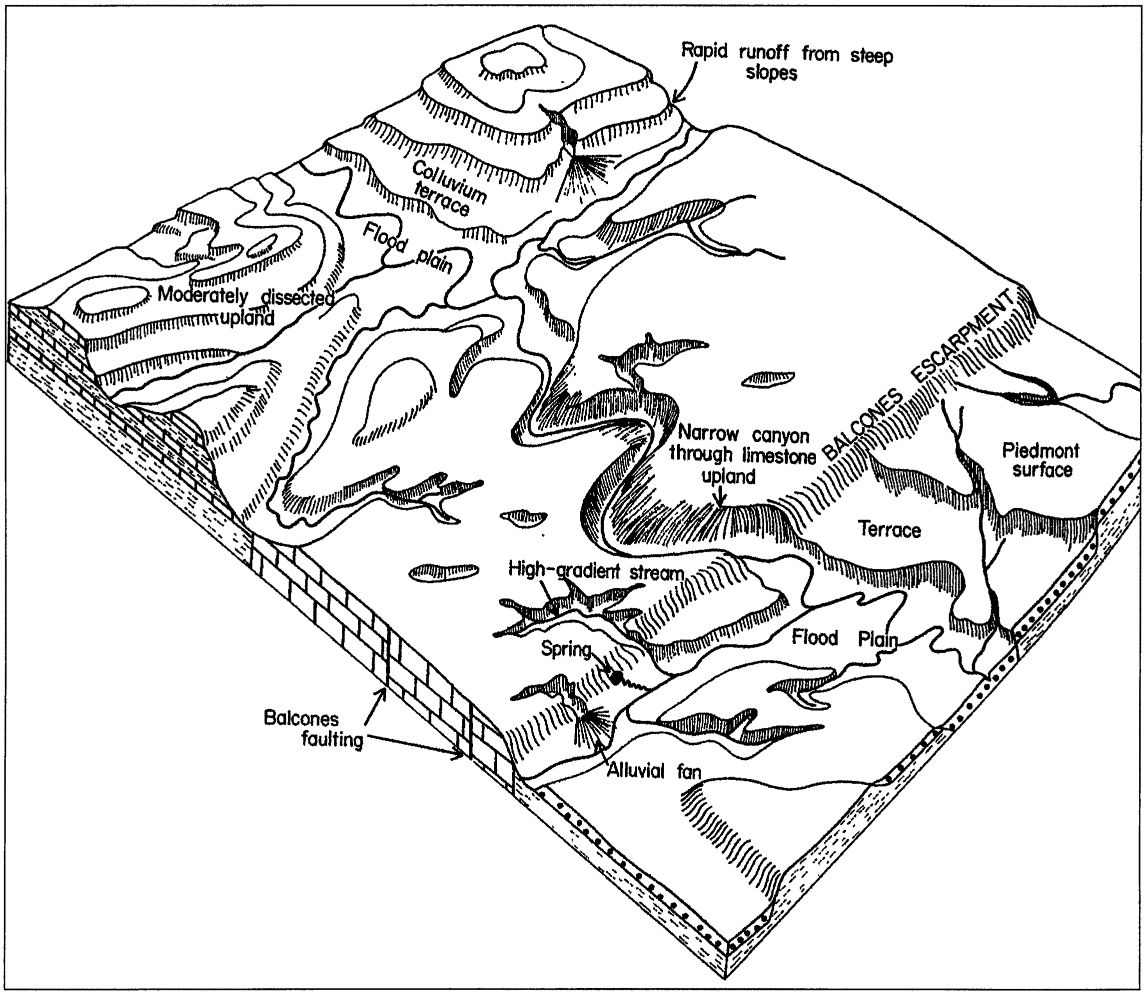

Fig. 2. Typical Edwards Plateau Geomorphology (Baker 1975)

The location and topography of this region combine to create a complex climate regime. In general, the climate of the Edwards Plateau straddles the subtropical steppe and subtropical savanna boundary (Swanson 1995, 46). The line that separates the subtropical steppe west from the humid subtropical east runs through the Edwards Plateau. Also, this imaginary line migrates back and forth annually (Hudson 2000). The mean annual precipitation on the plateau ranges from about 35.6cm (14in) at the western edge to 76.2cm (30in) along the Balcones Escarpment to the east (Swanson 1995, 46).

The second factor contributing to the highly variable climate on the plateau is the fact that the Balcones Escarpment rises up ninety-two meters from the low coastal plain, forming an abrupt barrier to moisture-laden air masses from the Gulf of Mexico. This tropical air is deflected upward resulting in orographic enhancement of the precipitation. This process can lead to powerful thunderstorms that tend to linger above the same location, resulting in huge accumulations of local rainfall (Petersen and Tuason 1995a, 12; Petersen and Tuason 1995b, 26; Swanson 1995, 157).

The unique combination of local climatological, topographic, and geologic factors associated with the south-central Texas region result in a serious flood risk making a knowledge of channel roughness values that much more important. Steep slopes, sparse vegetation, and thin soils are characteristic of the region. These natural conditions when exacerbated by human-induced processes such as overgrazing and increasing impervious surfaces result in extremely rapid runoff rates into streams. In addition, many local streams flow through narrow, resistant limestone canyons, which only serve to accelerate the already rushing floodwaters. The Edwards Plateau is clearly an area highly prone to very severe flood events (Baker 1975; Earl and Votteler 2002, 7; Petersen and Tuason

1995b, 26; Swanson 1995, 157). An accurate knowledge of channel roughness values is essential to predicting flood peaks and forecasting flood magnitudes.

CHAPTER IV

METHODOLOGY

Introduction

Because the roughness coefficient, *n*, cannot usually be measured directly, it must be estimated. Since Manning developed his model in the late 1800s, five major methods for generating values for *n* have been used commonly in the United States (Table 1). These methods require the collection of data either through direct measurements in the field or through those techniques utilizing visual estimates (Dingman and Sharma 1997, 15; Graf and Randall 1996, 6; Marcus et al. 1992, 228). This research combines data provided by the U.S. Geological Society (USGS) along with data collected in the field at selected streams on the Edwards Plateau to evaluate patterns of channel roughness and to determine locally accurate roughness estimates.

Data Collection

The USGS maintains numerous surface water and groundwater data collection gages in south-central Texas. The National Water Inventory System (NWIS), accessible through the USGS web site, provides numerous data on every stream gaging station in the entire United States. Included among these data are information on water quantity, water quality, and channel geometry at the gaging site. Of interest to this research are those gages where surface water measurements are recorded throughout the year. Fifty-one USGS gages on the Edwards Plateau satisfy these criteria (Figure 3). At each of these sites, data are collected on channel width, cross-sectional area, mean velocity, gage height, and streamflow (USGS 2002). For this research, at every gage site each of these channel measurements were recorded for three levels of flow: high, medium, and low. A flow level of "high", "medium", or "low" is a relative measure that changes for each gage. For each site the previous two years of data were analyzed and sorted to determine three distinct flow levels unique to each site.

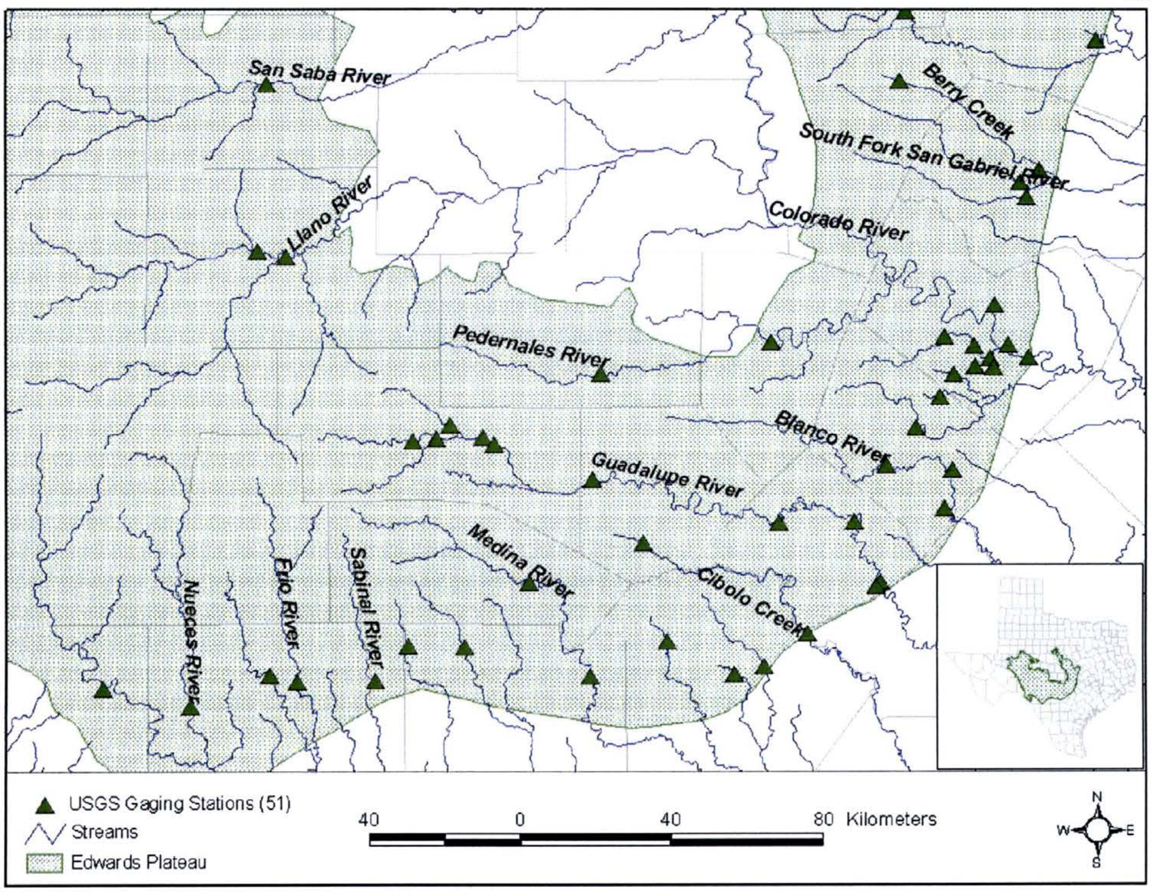

Fig. 3. USGS Gages on the Edwards Plateau (TPWD 2002, USGS 2002)

The USGS provided a great deal of useful data on water quantity and stream channel characteristics. However, using available USGS data in order to estimate roughness values required additional channel information, specifically channel slope and sediment size.

Channel slope is an essential physical parameter because of the large influence it has on streamflow velocity. The direct measurement of slope in the field, however, is time consuming and often problematic (Graf and Randall 1997, 75). Because slope calculations represent an average slope across an area buffering the actual gage site, determining slope from topographic maps is a proven acceptable method (Graf and Randall 1997, 75; Marcus et al. 1992, 228; Slade et al. 1995). In addition, the Manning equation determines velocity based on the square root of the slope thereby reducing the relative significance of slope measurement errors (Marcus et al. 1992, 228). For this research a local slope was measured for each gaging station directly from 1:24,000 USGS topographic maps using an opisometer (Graf and Randall 1997, 75; Slade et al. 1995).

The Limerinos and Bathurst equations required data on the distribution of sediment size across the channel. The most prevalent technique for collecting sediment size data in the literature is Wolman's (1954) pebble count method. The intermediate, or *b*, axis is measured for one hundred randomly collected particles across the stream channel in order to determine the eighty-fourth percentile (Fonstad 2000; Graf and Randall 1997, 46; Marcus et al. 1992, 223; Marcus et al. 1995, 2627; Phillips and Ingersol 1997, 155; Wolman 1954, 952). Collecting and measuring 100 random particles at each of fifty-one sites across south-central Texas proved to be beyond the time constraints of this thesis research. Therefore field data were collected at thirty-five of the gaging sites (Figure 4). At each of these sites the width of the channel was traversed, measured with a tape measure, and divided into thirty equal segments. The number thirty was chosen because it is the minimum number of measurements that can be taken in order to have a statistically significant sample size. The a-b-c dimensions of one clast per segment were measured using a Vernier caliper for use in the Limerinos and Bathurst equations, as well as in constructing a new equation from existing data. For samples too small to be measured with the caliper, particle size was approximated based on sediment type (Table 2).

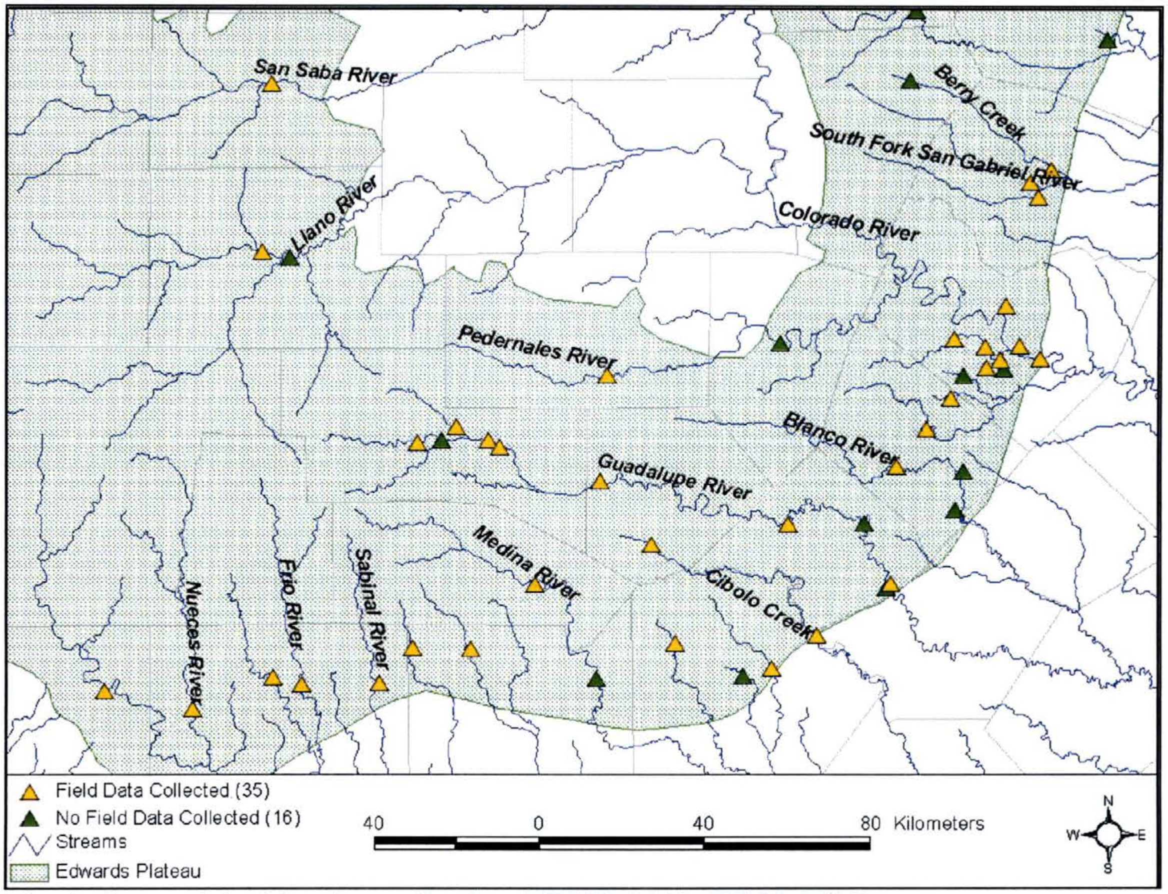

Fig. 4. Gages visited for data collection (TPWD 2002, USGS 2002)

Table 2. Particle size approximations (Singer and Munns 1991)

Soil Type	Particle Size (mm)
clay	0.0002
bedrock	0.0039
silty	0.0200
soft gritty sand	0 1000
loamy sand	0 2500
sand	0 5000
gritty sand	2 0000
concrete	2.0000
pea gravel	4 8077

In addition to sediment size data this research required visual estimates of roughness from each of the thirty-five sites in accordance with the USGS picture book method and Cowan's equation (Barnes 1967; Cowan 1956). Photos of streams of known roughness values were evaluated in the field, and the *n* value of the stream in the photo determined most similar to the channel in the field was recorded. Photographs taken in the field documented the accuracy of the comparisons (Figure 5). For Cowan's equation, each stream in the field was assessed in accordance with the constraints of the channel characteristics as shown in Table 3. Base roughness values (n_0) were taken from those values reported in Arcement and Schneider's water-supply paper (Table 4) (1989). The entirety of the data gathered at each gage site is presented in Appendix I.

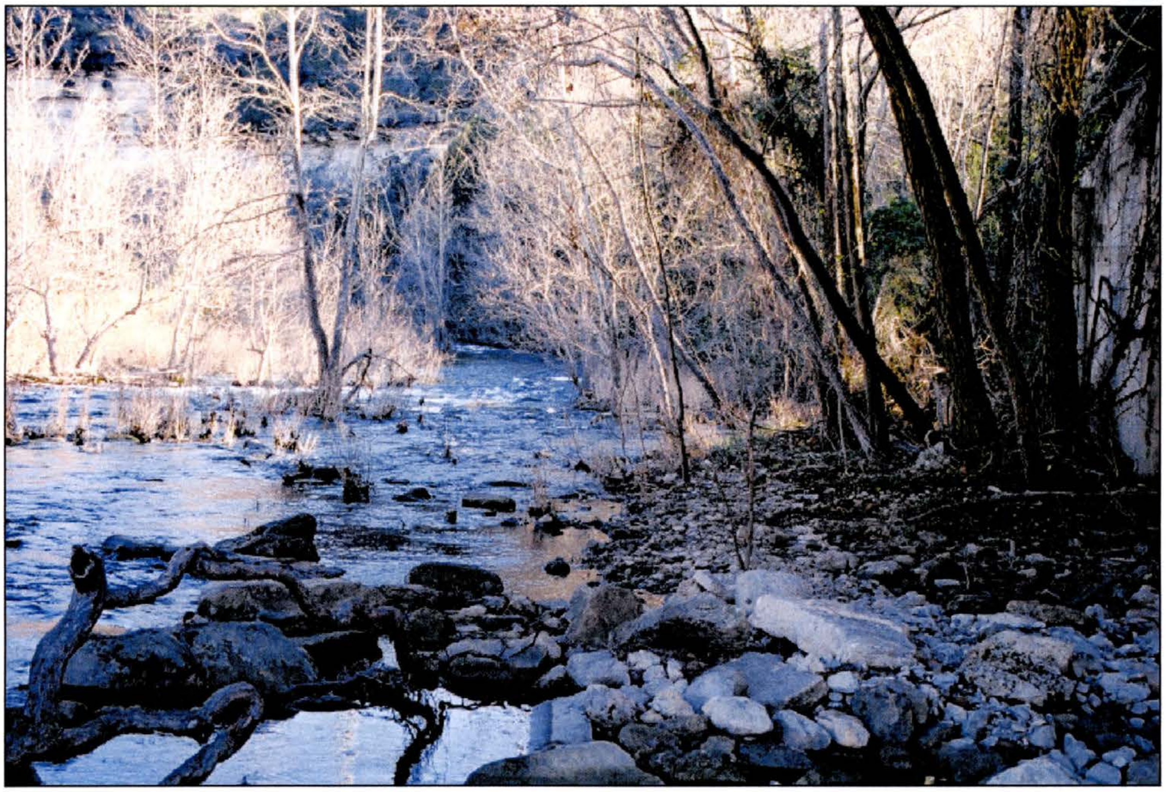

a.

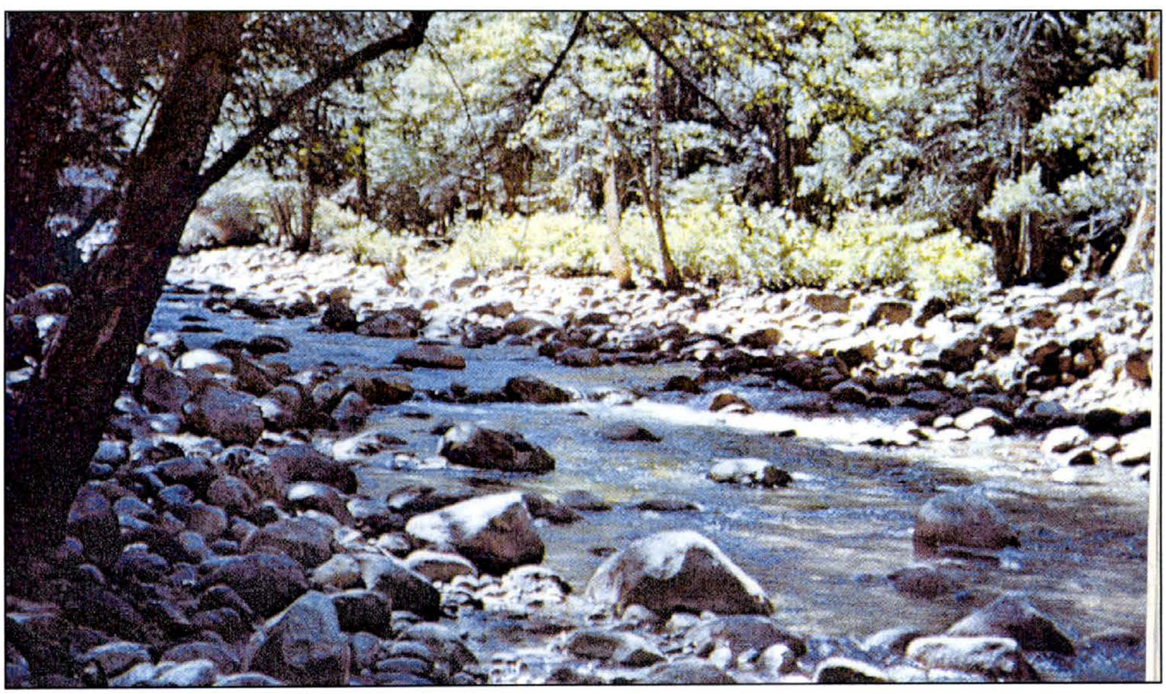

b.

Fig. 5. Comparison of photo (a) taken by author of Barton Creek at Lost Creek Boulevard to (b) picture book's Merced River near Yosemite, CA (Barnes 1967)

Table 3. Cowan's (1956) component method of estimating Manning's *n*

Channel Morphology and Conditions	Values
Sediment Type:	
Earth	0.02
Rock cut	0.025
Fine gravel	0.024
Coarse gravel	0.028
Degree of Irregularity:	
Smooth	0
Minor	0 005
Moderate	0 01
Severe	0.02
Variations in Cross Section:	
Gradual	0
Alternating occasionally	0 005
Alternating frequently	0 010-0.015
Effect of Obstructions:	
Negligible	0
Minor	0.010-0.015
Appreciable	0.020-0.050
Severe	0 040-0.060
Vegetation:	
Low	0.005-0.010
Medium	0.010-0 025
High	0.025-0 050
Very high	0.050-0.100
Degree of Meandering:	
Minor	1
Appreciable	1 15
Severe	1 3

Table 4. Base values of Manning's *n* (Arcement and Schneider 1989)

Bed material	Base *n* (n_0)
concrete	0 011
fine gravel	0 024
rock cut	0 025
coarse sand	0 026
coarse gravel	0.026
gravel	0.028
cobble	0.030
boulder	0 040

Data Transformation

Calculation of roughness estimates for the Edwards Plateau using the collected data required the computation of one remaining channel characteristic, specifically hydraulic radius. Hydraulic radius is a very important factor when determining roughness because it directly influences whether streamflow will be laminar or turbulent (Graf and Randall 1997, 45). The hydraulic radius of each channel is not measured by the USGS and direct measurement in the field is cumbersome and beyond the scope of this research (Graf and Randall 1997, 5; Tinkler 1997, 151). Derivation of this value from available data was therefore necessary.

Previous research addressed the use of depth as a substitute for hydraulic radius. Graf and Randall (1997) and Tinkler (1997) found that the accuracy of depth as a substitute for hydraulic radius depends most notably on the ratio of channel width to depth. In channels with width to depth ratios greater than twenty, the use of depth is considered most accurate. Large errors can occur with this substitution if the channel is relatively narrow and deep (Graf and Randall 1997, 5; Tinkler 1997, 151). The streams of interest for this research are generally wide and shallow; therefore, use of channel depth as a substitute for hydraulic radius when calculating channel roughness is possible.

Hydraulic radius is determined by dividing cross-sectional area by the wetted perimeter for each site. The area is given by the USGS, but wetted perimeter is not. How should the perimeter be calculated in order to determine a hydraulic radius value? The answer depends on how the channel shape is approximated. Fluvial geomorphologists use three basic shapes to approximate cross-sectional area: box, triangle, and parabola. Each shape employs a different formula to calculate area, incorporating width and some measure of depth. In addition, wetted perimeter can be determined for each shape.

Box Approximation of Channel Cross-section:

$$A_B = W * D_M$$
$$P_B = (2D_M) + W$$

Triangle Approximation of Channel Cross-section:

$$A_T = 0.5(W * D_M)$$
$$P_T = 2\sqrt{(0.5 * W)^2 + (D_M)^2}$$

Parabola Approximation of Channel Cross-section:

$$A_P = \frac{4(0.5 * W * D_M)}{3}$$
$$P_P = 2\left(\left(D_M\sqrt{1+\frac{W^2/8D_M}{2D_M}}\right)+\left(\left(\frac{W^2/8D_M}{2}\right) * \ln\left(\sqrt{1+\frac{2D_M}{W^2/8D_M}}+\sqrt{\frac{2D_M}{W^2/8D_M}}\right)\right)\right)$$

where A = cross-sectional area, P = wetted perimeter, W = channel width, and D_M = maximum depth.

Gage height is assumed to be strongly correlated to maximum depth. This research hypothesized the gage height given by the USGS was approximately equal to maximum depth. The most accurate shape approximation for three flow levels at each of the fifty-one gaging sites was determined by computing area using each of the three shape formulas and comparing these values to the measured area given by the USGS. Once the most appropriate shape was revealed, wetted perimeter was calculated. Finally a hydraulic radius value was calculated based on the USGS area measure and the derived perimeter value.

Previous research by Fonstad (2000) and Robison and Beschta (1989) tested channel shape approximations as predictors of several channel characteristics. Both studies analyzed measurements of bankfull width and thalweg depth taken across highly detailed cross-sections and compared them to those values determined using channel shape approximations (Fonstad 2000, 102-108; Robison and Beschta 1989, 191). Fonstad tested the box and the triangle shape approximations and found that both tended to underestimate channel velocity. His research also determined that the box shape produced more accurate approximations of depth and hydraulic radius than the triangle shape (Fonstad 2000, 102-108). Robison and Beschta (1989) tested only the triangle shape and found that there was no significant difference between actual and approximated cross-sectional areas for each of their more than three hundred sites (Robison and Beschta 1989, 191). The triangle shape provided the most accurate area approximation for this research. For the streams with a low or medium flow level the triangle shape was most appropriate for eighty-six percent of the sites (eighty-eight sites total). For high flows the triangle approximation was used for seventy-five percent of the hydraulic radius calculations.

CHAPTER V

ANALYSIS OF THE DATA

Introduction

In order to answer the three research questions the data used for this study had to be highly organized, easily accessible and clearly labeled. Therefore downloaded data from the USGS-NWIS as well as those data collected in the field were entered into spreadsheets in Microsoft Excel. Once entered, all data were converted to metric units and readied for analysis. The entirety of the gage data used for the analysis is presented in Appendix II.

Observed Roughness Values

Observed roughness values were calculated for all three flow levels at each of the fifty-one gage sites using velocity values from the USGS, hydraulic radius values calculated using area approximations, and slope values measured from topographic maps. This was done using the equation builder function in Excel and with a variation of the Manning equation given below.

$$n = \frac{R^{2/3} S^{1/2}}{v} \tag{5}$$

These observed roughness values were then added as a table in ArcView 3.2. A map was created for each of the three flow levels in order to determine whether a pattern of roughness values on the Edwards Plateau emerged (Figures 6-8). This analysis revealed no clear pattern of roughness across the study area for any flow level. Observed values of roughness differed between drainage basins as well as among gages on the same stream.

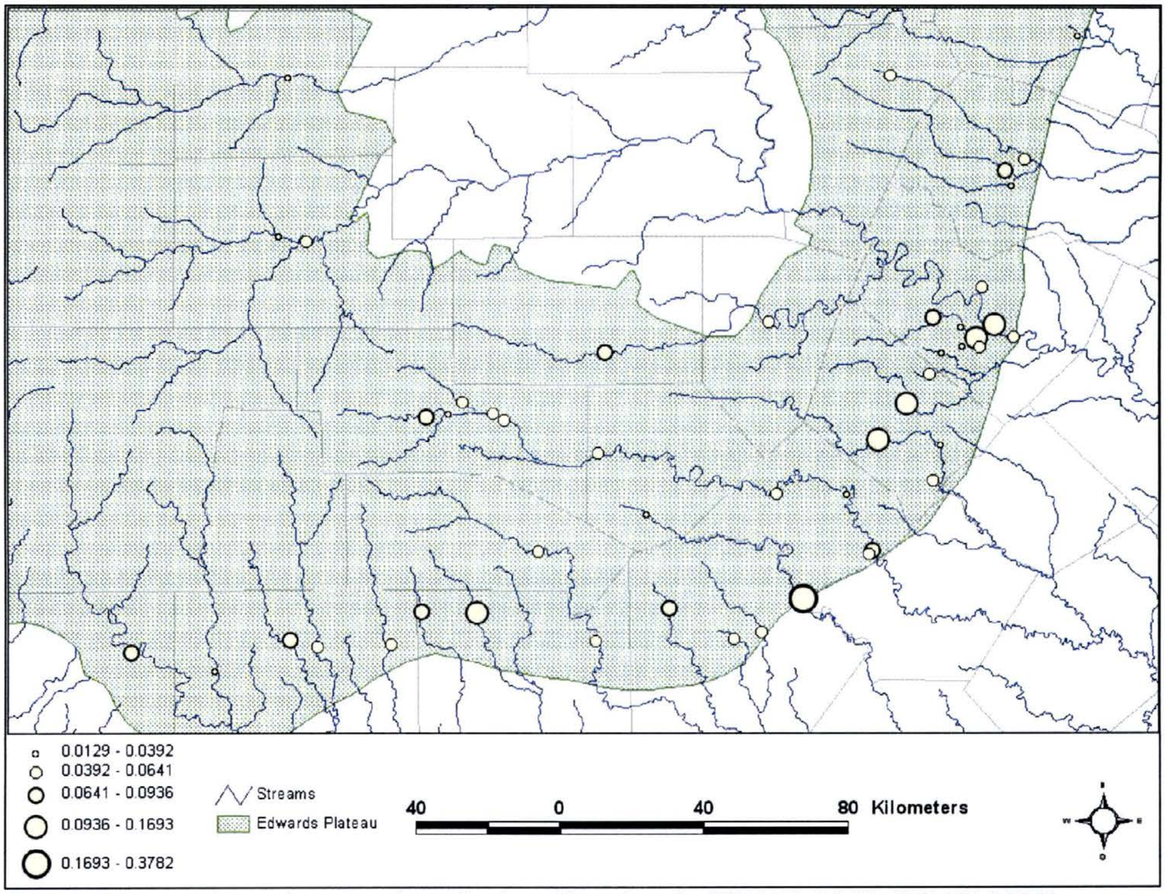

Fig. 6. Observed roughness values for low flow levels (TPWD 2002, USGS 2002)

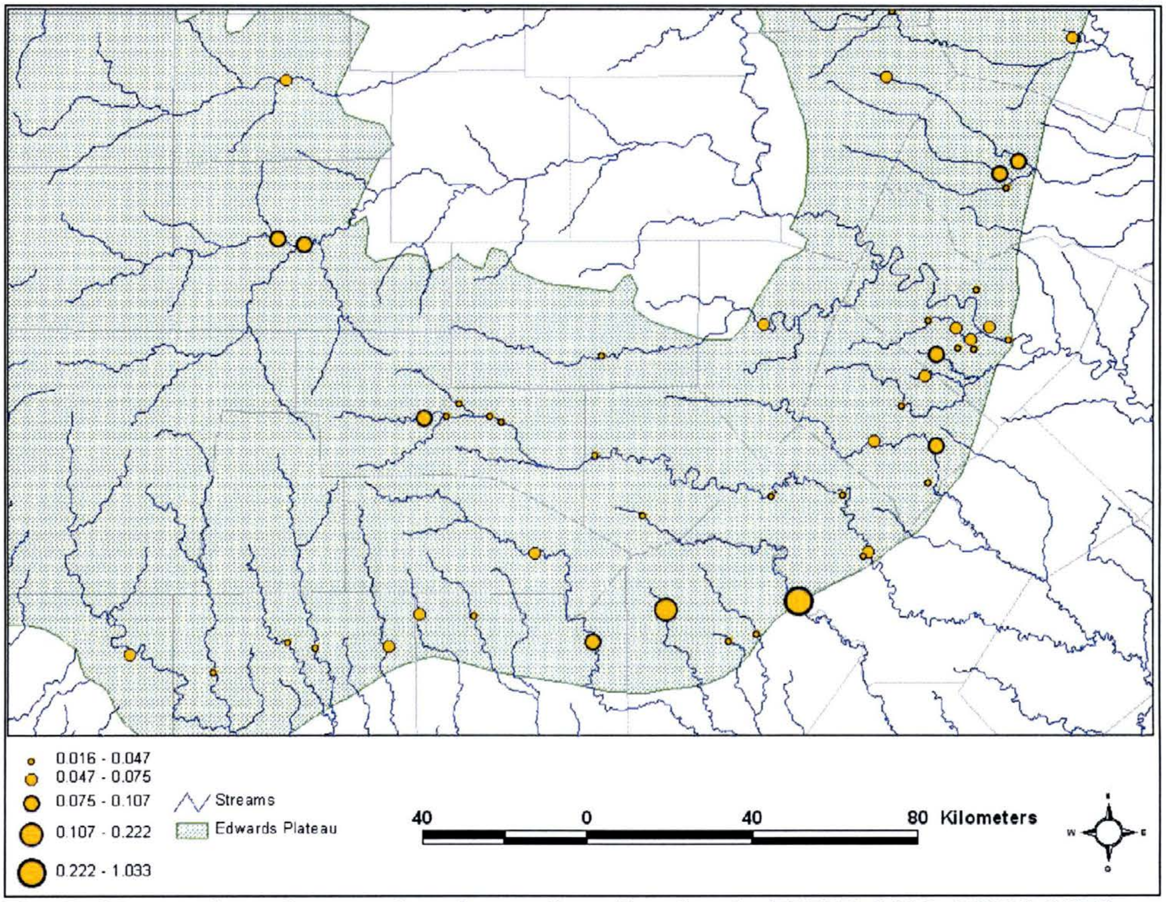

Fig. 7. Observed roughness values for medium flow levels (TPWD 2002, USGS 2002)

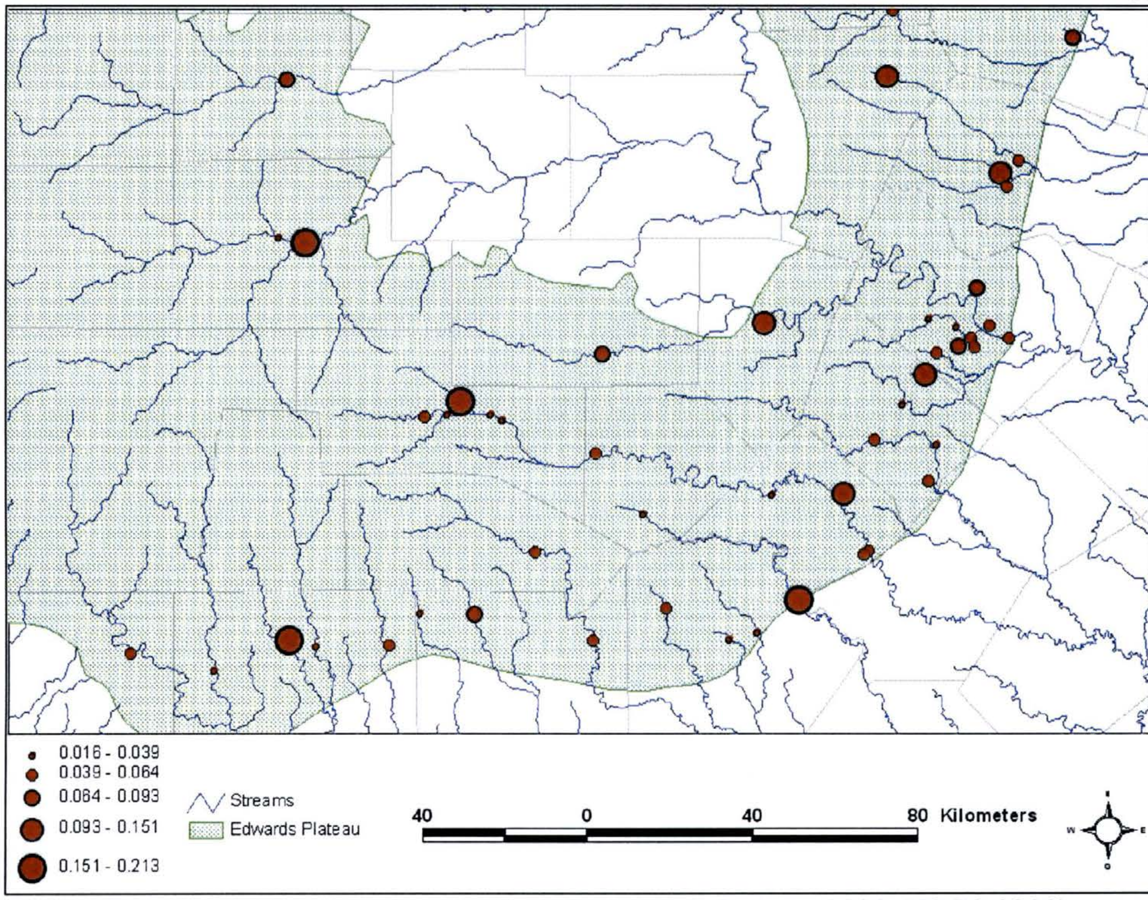

Fig. 8. Observed roughness values for high flow levels (TPWD 2002, USGS 2002)

Predicted Roughness Values

Determination of which published equation best predicted *n* required further analysis. First, the three equations requiring mathematical calculations – the Bathurst, Limerinos, and Jarrett equations – were input into Excel to produce roughness estimates. Note that roughness values predicted from the USGS picture book method and Cowan's equation required no calculations and were input directly from field data notes. For each flow level for the thirty-five gages where field data were collected the five predicted roughness values were compared to observed values using simple linear regression. In addition, the data were split into two separate categories based on channel substrate. Of the thirty-five streams visited twenty-one flow over some amount of exposed limestone bedrock and fourteen were strictly alluvium channels. The linear regression tests for each predicted value versus observed value were rerun on the separated data (Table 5).

Table 5. Observed v. predicted roughness values

		LOW FLOW			MEDIUM FLOW			HIGH FLOW		
		r2	**y-int**	**slope**	**r2**	**y-int**	**slope**	**r2**	**y-int**	**slope**
ALL	Bathurst	0 0101	0.0466	-0 0453	0.0907	0.0378	-0.0226	0 0090	0.0335	-0.0188
	Cowan	0 0645	0.0626	-0 1445	0.0069	0 0532	-0.0174	0.0084	0.0474	0 0656
	Jarrett	0.0081	0 0834	-0 0323	0.0176	0.0724	-0.0122	0.0092	0.0634	0 0279
	Limerinos	0.0167	0.0645	-0.1058	0 0879	0.0429	-0.0278	0.0107	0 0370	-0.0241
	USGS	0.0018	0 0382	0.0069	0.0510	0 0376	0.0134	0.0059	0.0377	0.0156
Bedrock	Bathurst	0 0032	0.0313	0.0189	0.0932	0 0358	-0.0208	0.0016	0.0294	0.0076
	Cowan	0 0737	0.0636	-0.1428	0.0101	0.0564	-0 0177	0.0222	0.0442	0.0953
	Jarrett	0.0703	0 0930	-0 0919	0.0677	0.0782	-0.0182	0 0014	0.0690	0.0091
	Limerinos	0.0007	0.0384	0 0106	0 0933	0.0407	-0.0257	0 0009	0.0323	0.0067
	USGS	0.0365	0 0366	0.0246	0.1056	0.0372	0.0140	0 0094	0 0375	0.0152
Alluvium	Bathurst	0.0456	0 0673	-0.1397	0 0022	0 0402	-0.0160	0 3191	0.0430	-0.1442
	Cowan	0 0509	0.0630	-0.1773	0.0000	0.0516	0.0090	0.0204	0.0631	-0 2193
	Jarrett	0 1614	0.0649	0 1580	0 0204	0 0592	0.0804	0.0694	0.0658	-0.1450
	Limerinos	0 0380	0.1017	-0.3135	0.0043	0.0460	-0.0298	0 3244	0.0485	-0.1827
	USGS	0.0787	0 0435	-0 0779	0 0033	0 0403	-0.0280	0.0049	0.0368	0 0380

None of the published equations successfully or consistently predicted roughness at a significant level. The Limerinos equation produced the highest coefficient of determination (r^2) value of 0.32 for alluvial channels with a relatively high flow. Bathurst's equation was very close behind with an r^2=0.31 for the same channel substrate and level of flow. Jarrett's equation provided the third highest r^2 value of 0.16 for alluvial channels with relatively low flow. The roughness values of the remaining flow levels and varying substrate types could only explain less than 10% of the variance.

Though none of these prediction equations produced accurate roughness estimates, each was consistent in relative over or under-prediction as shown in Figures 9-11. The Bathurst equation under-predicted roughness in seventy-five percent of the cases at all three levels of flow. Cowan's equation also under-predicted roughness at twenty-five of the thirty-five gage sites. Jarrett's equation was the only method tested by this research that did not under-predict roughness. At all three flow levels, this equation resulted in a calculated *n* higher than the observed value in two-thirds of the cases. For the low and high flow levels the Limerinos equation under-predicted in a large majority of the cases (~75%). For medium flows this equation again under-predicted roughness but in slightly less cases (~63%). The USGS picture book method under-predicted roughness at eighty percent of the gage sites for all three levels of flow. Clearly these five commonly used prediction methods do not yield valid roughness values for the many streams in this study area.

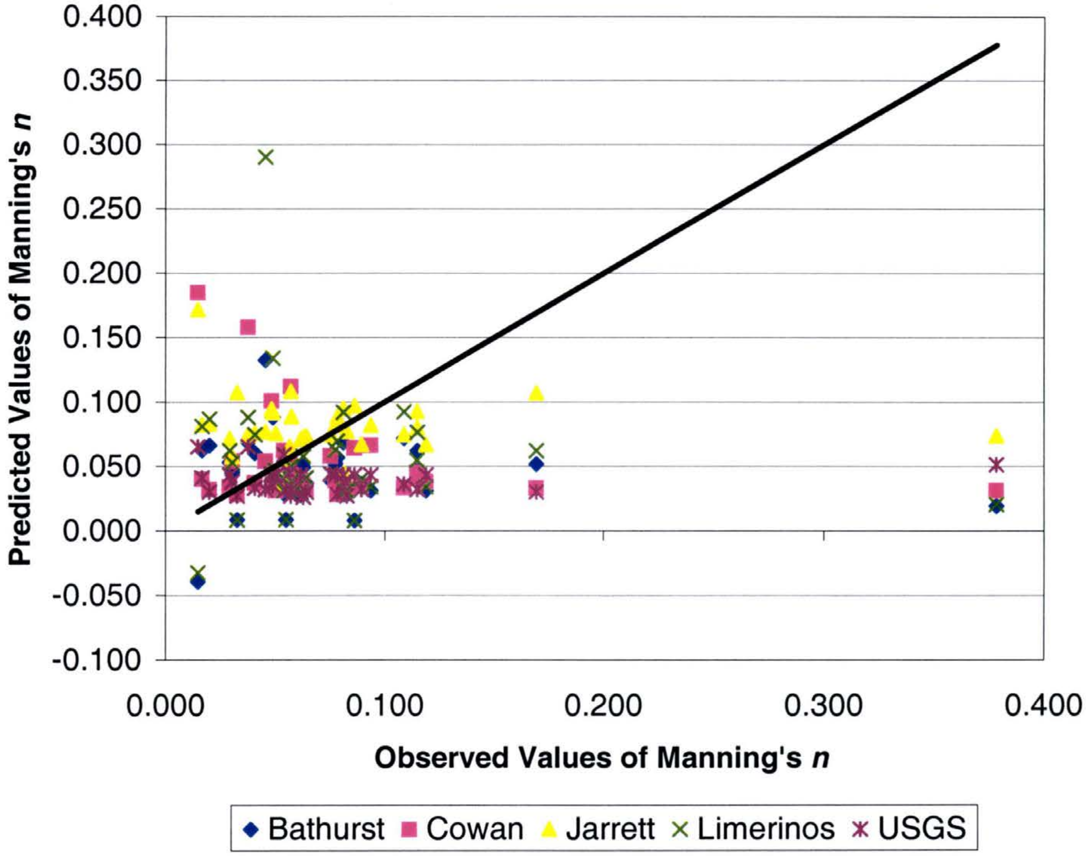

Fig. 9. A comparison of observed roughness and estimated roughness for low flow streams. The solid line indicates the line of perfect agreement.

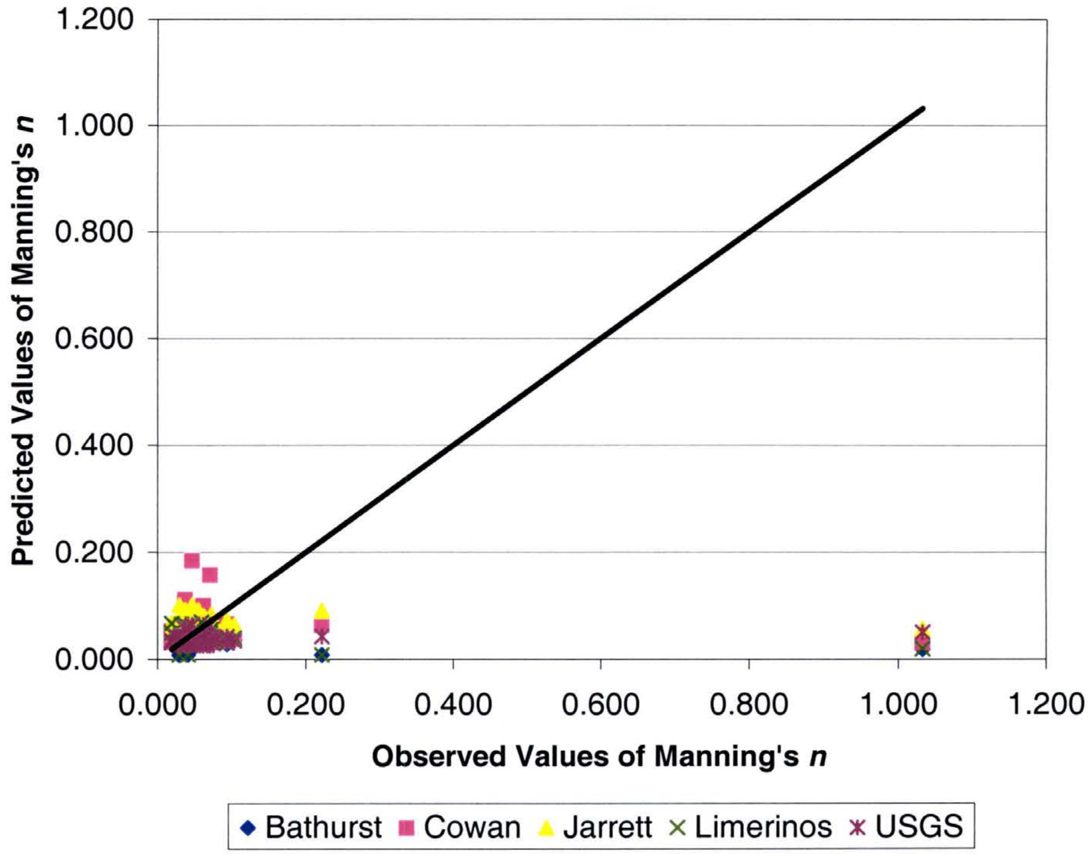

Fig. 10. A comparison of observed roughness and estimated roughness for medium flow streams. The solid line indicates the line of perfect agreement.

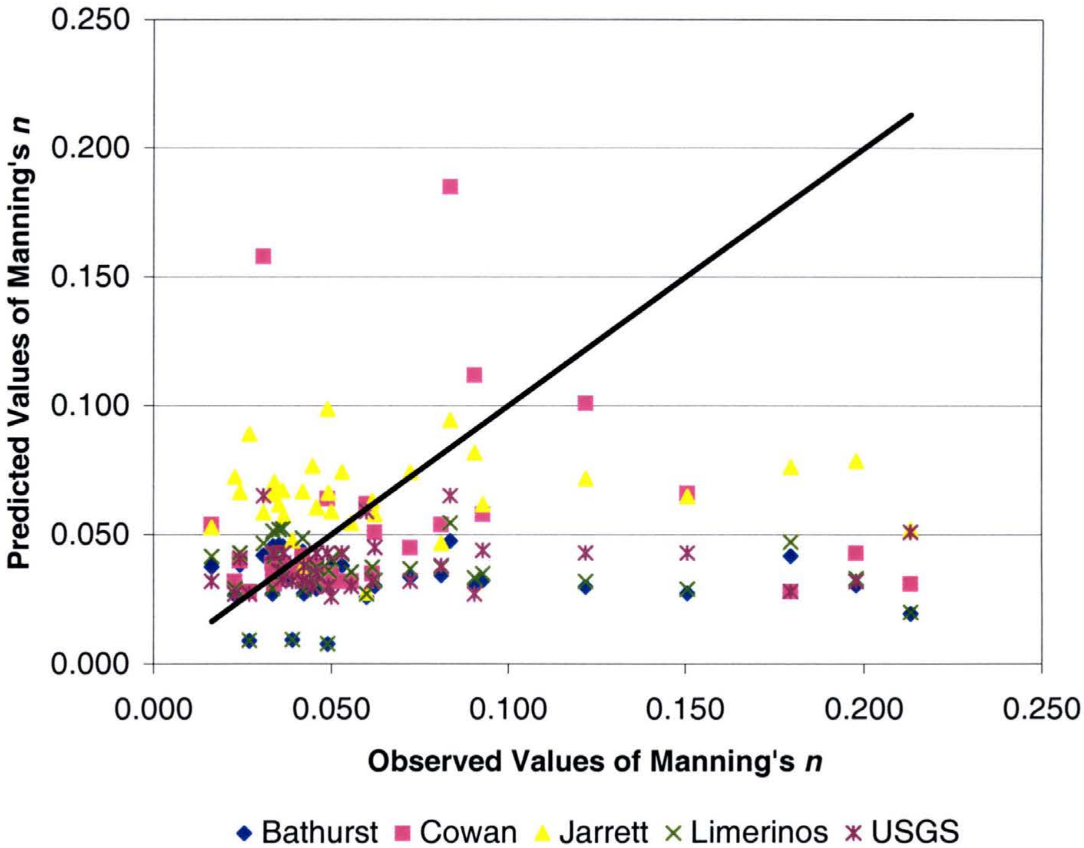

Fig. 11. A comparison of observed roughness and estimated roughness for high flow streams. The solid line indicates the line of perfect agreement.

New Prediction Equations

Because those equations tested in this study were unsuccessful in predicting accurate roughness values it was necessary to generate new prediction equations. The first and most common method of generating such equations utilized SPSS to build linear regression models. Data on observed roughness (*n*), hydraulic radius (r), slope (s), maximum depth (d_{max}), width-to-depth ratio (w-d), sediment size (d_{84}), and substrate for each flow level for the thirty-five gages were input into SPSS. Histograms displayed the normality of the data. In the event that a variable did not appear to be normal data transformations were utilized. Separate multiple linear regressions were run for all the bedrock channels and all the alluvial channels using r, s, d_{max}, w-d, and d_{84} as the independent variables in an effort to predict observed roughness (*n*). This process was repeated with the data separated this time by not only substrate but flow level as well. None of these linear regressions explained more that 50% of the relationship between predicted and observed roughness (Table 6).

Table 6. Validity of new prediction equations using SPSS

Substrate	Flow Level	r^2
Alluvium	All	0.189
	Low	0.493
	Medium	0.171
	High	0.284
Bedrock	All	0.151
	Low	0.285
	Medium	0.446
	High	0 476
Both	Low	0.251
	Medium	0 392
	High	0 400

Successfully answering the third research question required hypothesizing nonlinear predictive equations. This research employed the tool in Microsoft Excel known as 'Solver', which obtains a best fit to a proposed equation by minimizing the root mean square of the model to a data set. Three equation forms were modeled after those developed by Jarrett, Bathurst and Limerinos, and Tinkler (Table 7) (Bathurst 1985; Jarrett 1984; Limerinos 1970; Tinkler 1997). The remaining forms were created based on available data from this study and following the exponential form of Jarrett's and Tinkler's equations.

Table 7. Results of new prediction equations using Solver

		r^2 values		
		LOW	MED	HIGH
Solver 1 (Jarrett)	Both	0 0944	0.9526*	0 1736
$y = a * S^b * R^c$	Bedrock	0 0404	0.9590*	0 3150
	Alluvium	0.7525	0 1888	0.1520
Solver 2 (Bathurst & Limerinos)	Both	0 0007	0.9499*	0 0521
$y = \frac{a * R^b}{c + d * \log(R / d_{84})}$	Bedrock	0 0019	0 9564*	0.0957
	Alluvium	0.1282	0.1563	0.1836
Solver 3 (Tinkler)	Both	0 0131	0.0094	0 0721
$y = a * S^b * d_{max}{}^c$	Bedrock	0.0348	0.0195	0.0818
	Alluvium	0 6602	0.0800	0 0156
Solver 4	Both	0 0341	0.0072	0 1563
$y = a * S^b * w - d^c$	Bedrock	0.0358	0.0058	0 1862
	Alluvium	0 6693	0.0780	0 0600
Solver 5	Both	0 0129	0.0268	0.0772
$y = a * S^b * d_{84}{}^c$	Bedrock	0 0345	0 0185	0.1146
	Alluvium	0 6625	0 0788	0.2002
Solver 6	Both	0 0489	0.9524*	0 0521
$y = a * R^b * d_{84}{}^c$	Bedrock	0.0368	0 9564*	0 0976
	Alluvium	0.1401	0.1780	0.2083

*see Chapter V for discussion of these high r^2 values

Predicted *n* values produced by these equations were compared to observed roughness values through simple linear regression. Equations 6, 7 & 8 each provided exceptional r^2 values of 0.95 for all thirty-five field gage sites with a relatively medium flow. Shown below are those equations (6-8) with the determined coefficients included.

$$n = 2.25 S^{-0\;26} R^{19} \tag{6}$$

$$n = \frac{11 R^{16}}{2.7 - 0.5 \log(R / d_{84})} \tag{7}$$

$$n = 0.05 R^{0\;12} d_{84}^{\;-0\;07} \tag{8}$$

These exceptionally high r^2 values are discussed in Chapter V. None of the hypothesized predictive equations produced significant roughness values for the low or high flow levels and for both substrate types. Several predictive equations had high r^2 values but only for either bedrock or alluvial channels. Since each of these data sets had less than thirty observations, the equations' r^2 values cannot be considered significant.

CHAPTER VI

DISCUSSION OF RESULTS AND CONCLUSION

If patterns of roughness existed and were evident across the Edwards Plateau it might be possible to better estimate velocity in times of flood or simply on streams without gages where knowledge of streamflow might benefit an agricultural land management strategy. For low, medium, and high flow levels at the fifty-one gages in the study area, a roughness value was calculated and mapped (Figures 6-8). Unfortunately it appears from the analysis completed in this research that no such simple pattern exists. It appears that the many intricate factors that affect roughness differ enough across the study area as to prevent any similarity among streams in the same basin or even different locations along the same river.

Studies completed previously revealed the difficulties in predicting n and produced various equations and methods attempting to do just that. However none of these studies suggested a means to estimate channel roughness in the state of Texas or more specifically on the Edwards Plateau. Over the years five models emerged as the most commonly applied estimation techniques and these were tested for data collected both from the USGS and from the field for selected south-central Texas streams. Prediction methods developed by Bathurst, Cowan, Jarrett, Limerinos, and the USGS all failed to produce accurate estimates in this area.

The Bathurst and Limerinos equations are intended for use on channels where bed material is the primary source of roughness. Because streams in this study flow over various substrates, namely alluvium or bedrock, no generalization can be made about bed material as the primary source of roughness. Also the Bathurst equation is intended for channels with slope values greater than 0.004 (Bathurst 1985; Marcus et al. 1992, 229). Only seven out of fifty-one streams in this study had slope values greater than or equal to that value. Testing these equations against observed roughness values provided evidence in accordance with these limitations. Separating the data into categories based on substrate and retesting the equations provided r^2 values around 0.30, which are hardly high coefficients of determination. In addition, the size of the sample was less than thirty for the retesting such that the merit of these equations as significant predictors of roughness is further questionable.

The USGS photographic approach is clearly the simplest and most inexpensive method for predicting roughness. It is intended for one depth of flow, usually near bankfull, and is generally inappropriate for other flow levels (Barnes 1967; Marcus et al. 1992, 228). This seems to be at least partly evident after trying the method in this research. The USGS picture book method tested best for bedrock channels with a medium flow. However the r^2 value was hardly impressive at 0.10, and again the size of the sample was only twenty-one. Because pictures were taken at each of the thirty-five field sites, a new reference now exists for streams in this region that might be useful for predicting *n* on the Edwards Plateau. The existing book, however, does not predict roughness accurately well in south-central Texas.

Cowan's method for predicting *n* is also simple and inexpensive. His component approach requires only visual observations and requires no field measurements (Cowan 1956; Marcus et al. 1992, 229). Like the USGS picture book method, however, user inexperience can greatly affect the success of this method in producing both consistent and accurate results. Cowan's equation produced varying results in this study. No r^2 value exceeded 0.07 when comparing observed to predicted values. User inexperience may have played a role in the poor predictive ability of Cowan's equation in south-central Texas, or perhaps this component approach simply is not applicable in this study area.

Jarrett's equation also failed to produce statistically significant predicted *n* values. This equation is intended for hydraulic radius values between 0.15 and 2.1 meters and slopes between 0.002 and 0.04 (Jarrett 1984; Marcus et al. 1992, 229). The slope values in this study fit within the constraints, but twenty-five percent of the hydraulic radius values fall below the suggested length. This may have led to the poor *n* estimates produced by Jarrett's equation. The highest r^2 achieved was 0.16 for alluvial channels with low flows. As stated previously Jarrett's equation relates slope to hydraulic radius, and neither of those variables were collected in the field for this study. Perhaps this fact resulted in the equation failing to provide accurate estimates of channel roughness.

The need to develop a nonlinear equation based on data collected for this study is evidenced by the poor regression equations that resulted from the SPSS analysis and were discussed in chapter four. The significance of the success of the three hypothesized equations for medium flow levels is surprising. Coefficients of determination of 0.95 are rare and especially suspect when compared to the dismal relationships discovered previously in the analysis. Both new equations significantly predicted *n* for medium flows for both substrate types together and also successfully predicted *n* for the bedrock channels with a medium flow. These equations were modeled after Jarrett's, Bathurst's and Limerinos' equations.

Further examination of the predicted roughness values of these new equations revealed a simple explanation. Upon closer inspection it was apparent that the predicted roughness of one site in particular (Cibolo Creek at Selma) was almost exactly equal to the observed roughness as calculated by these three new equations. This nearly perfect prediction skewed the regressions which resulted in the extremely high r^2 values. Removing this site from the data and resolving for *n* led to more realistic r^2 values that were similar to those given earlier in the analysis. Equations 6, 7, and 8 produced r^2 values of 0.0009, 0.1800 and 0.1852 respectively for medium flows without the Cibolo Creek at Selma data. While these numbers are not as grand as those thought to be correct previously, equations 7 and 8 still provided the highest r^2 values of any of the new prediction equations. It cannot be said that deriving a new equation for predicting roughness was a success. It is important to note, however, that the two most successful equations relate sediment size and hydraulic radius in order to predict roughness. This research may provide cause to further explore this relationship.

Future Research Possibilities

The time constraints of this thesis research limited the amount of gage sites that could be visited for data collection. This resulted in a sample size of thirty-five, which on its own is of significant size. When broken down into categories based on substrate, though, the sample sizes drop to twenty-one and fourteen, which are no longer significant. A larger amount of data might have benefited this study. However it is important to note that with a total of only fifty-one gages on the Edwards Plateau, visiting them all for field data still would have resulted in at least one category still having too few samples. Perhaps a larger study area might result in a large enough sample size based on the criteria of this study. Also if the data were all collected in the field rather than relying on the USGS-NWIS gage site data, the sample size would be more easily increased while maintaining the Edwards Plateau as the focus area of the research.

Further research on this topic might include a collection of large amounts of data in two distinct river basins in Texas in order to compare roughness values over large areas. Also this data could be used to test the two prediction equations hypothesized in this research in order to examine their validity on other streams and in other regions. Because large amounts of data were collected for this study, further calculations using these data on fluvial topics such as width to depth ratios and historic flood peaks might be completed. An additional study might use the pictures taken for this study in the field to predict roughness and determine whether they provide valid results.

Conclusion

Although the Edwards Plateau is considered a natural region in Texas comprised of an area with common characteristics such as geology, soils and topography, the land features are certainly not homogenous. Small variations in things like riparian vegetation or local slope, as well as the presence or absence of man made features, can greatly alter the structure of a channel and consequently its roughness. Roughness is affected by deviations in flow depth, sediment load, particle size, vegetation, other obstructions, and interactions between these factors (Dingman and Sharma 1997, 15; Graf and Randall 1997, 45; Knighton 1998, 101; Marcus et al. 1992, 228). The complexities of estimating *n* values are well documented for streams outside Texas, and this research provides further evidence to that same end based on a selection of streams on the Edwards Plateau.

When a stream gage is not present or not functioning properly it may be necessary to estimate velocity and discharge. Knowledge of a channel's roughness is essential to correctly predict river velocity and thus discharge. Because roughness cannot be measured directly, it must be estimated using any number of previously discussed methods. The purpose of this research was to investigate roughness estimates and their ability, or in this case inability, to accurately predict roughness. The results provide insight into the difficulty associated with the task of assigning an *n* value to a stream on the Edwards Plateau. Fieldwork played a vital role in this research, and the value of getting out and experiencing the physical environment was strengthened. Studying the constantly changing patterns of our surroundings allows us to interpret the world around us as geographers.

APPENDIX I

GAGING STATION DATA

Data presented in Appendix I represents data used to calculate observed roughness and predicted roughness values for each of the fifty-one gaging stations in this study. Gages visited in the field also include photographs taken by the author. Those data marked with a superscript 1 were gathered by the author, a 2 signifies data collected from the USGS-NWIS website, and a 3 denotes values that were calculated from available data.

08101000 Cowhouse Creek at Pidcoke, Tx
31.2847°N, 97.8847°W

	Low	Medium	High
Slope[1]	0.0018	0.0018	0.0018
XS Area[2]	0.3869	1 5438	11 4390
D_{max}[2]	0 9266	1.0759	1.5149
Velocity[2]	0.2073	0 9022	0.9632
Radius[3]	0 0832	0.2025	0.4544
d_{84}[1]	n/a	n/a	n/a
w-to-d[3]	4.6053	6 7989	16 4990
$n_{observed}$	0 0392	0.0163	0.0262
Bathurst	n/a	n/a	n/a
Cowan	n/a	n/a	n/a
Jarrett	0 0771	0.0669	0 0587
Limerinos	n/a	n/a	n/a
USGS	n/a	n/a	n/a

08103800 Lampasas River near Kempner, TX
31.0817°N, 98.0164°W

	Low	Medium	High
Slope[1]	0 0022	0 0022	0.0022
XS Area[2]	1.9716	4 8360	14.0430
D_{max}[2]	1.1034	1.1826	1.4569
Velocity[2]	0.3170	0.5395	0 7772
Radius[3]	0 1198	0 2388	0.5547
d_{84}[1]	n/a	n/a	n/a
w-to-d[3]	14 7790	17 0103	17 2594
$n_{observed}$	0 0361	0.0336	0.0409
Bathurst	n/a	n/a	n/a
Cowan	n/a	n/a	n/a
Jarrett	0 0775	0.0694	0.0607
Limerinos	n/a	n/a	n/a
USGS	n/a	n/a	n/a

08103900 South Fork Rocky Creek near Briggs, TX
30.9114°N, 98.0367°W

	Low	Medium	High
Slope[1]	0.0045	0.0045	0.0045
XS Area[2]	0 3534	2 3343	11.4390
D_{max}[2]	0 4084	0 6645	0.9571
Velocity[2]	0.2134	0.4755	0 5243
Radius[3]	0.0813	0.2800	0.8288
d_{84}[1]	n/a	n/a	n/a
w-to-d[3]	10.4478	12.3853	12.4204
$n_{observed}$	0.0589	0.0603	0.1127
Bathurst	n/a	n/a	n/a
Cowan	n/a	n/a	n/a
Jarrett	0.1033	0.0847	0.0712
Limerinos	n/a	n/a	n/a
USGS	n/a	n/a	n/a

Lampasas River near Belton, TX
31.0017°N, 97.4922°W

	Low	Medium	High
Slope[1]	0.0023	0.0023	0.0023
XS Area[2]	1.1532	8.7792	46.6860
D_{max}[2]	1.5484	1 8745	3.0175
Velocity[2]	0 3200	0.4389	0 7346
Radius[3]	0 1170	0.3840	1.3467
d_{84}[1]	n/a	n/a	n/a
w-to-d[3]	6 0433	12.0325	11.3131
$n_{observed}$	0.0357	0.0575	0.0794
Bathurst	n/a	n/a	n/a
Cowan	n/a	n/a	n/a
Jarrett	0.0785	0.0649	0.0531
Limerinos	n/a	n/a	n/a
USGS	n/a	n/a	n/a

08104700 North Fork San Gabriel River near Georgetown, TX
30.6617°N, 97.7111°W

Downstream view from left bank

	Low	Medium	High
Slope[1]	0.0033	0.0033	0.0033
XS Area[2]	0.9486	4.2129	21.4830
D_{max}[2]	1.4173	1.6642	2.0422
Velocity[2]	0.2073	0.3109	0.3383
Radius[3]	0.1947	0.3583	0.8286
d_{84}[1]	0.0407	0.0407	0.0407
w-to-d[3]	2.7957	6.7766	12.5373
$n_{observed}$	0.0936	0.0937	0.1505
Bathurst	0.0311	0.0289	0.0273
Cowan	0.0660	0.0660	0.0660
Jarrett	0.0817	0.0741	0.0648
Limerinos	0.0341	0.0312	0.0290
USGS	0.0430	0.0430	0.0430

08104900 South Fork San Gabriel River at Georgetown, TX
30.6256°N, 97.6908°W

Upstream view of left bank

	Low	Medium	High
Slope[1]	0.0020	0.0020	0.0020
XS Area[2]	0.1869	2.9946	22.1340
D_{max}[2]	0.7498	0.9540	1.5636
Velocity[2]	0.3536	0.4846	0.7376
Radius[3]	0.0630	0.2925	0.8787
d_{84}[1]	0.0931	0.0931	0.0931
w-to-d[3]	3.4146	10.5431	15.9844
$n_{observed}$	0.0200	0.0407	0.0556
Bathurst	0.0661	0.0383	0.0330
Cowan	0.0320	0.0320	0.0320
Jarrett	0.0831	0.0650	0.0545
Limerinos	0.0867	0.0427	0.0355
USGS	0.0300	0.0300	0.0300

08105100 Berry Creek near Georgetown, TX
30.6911°N, 97.6558°W

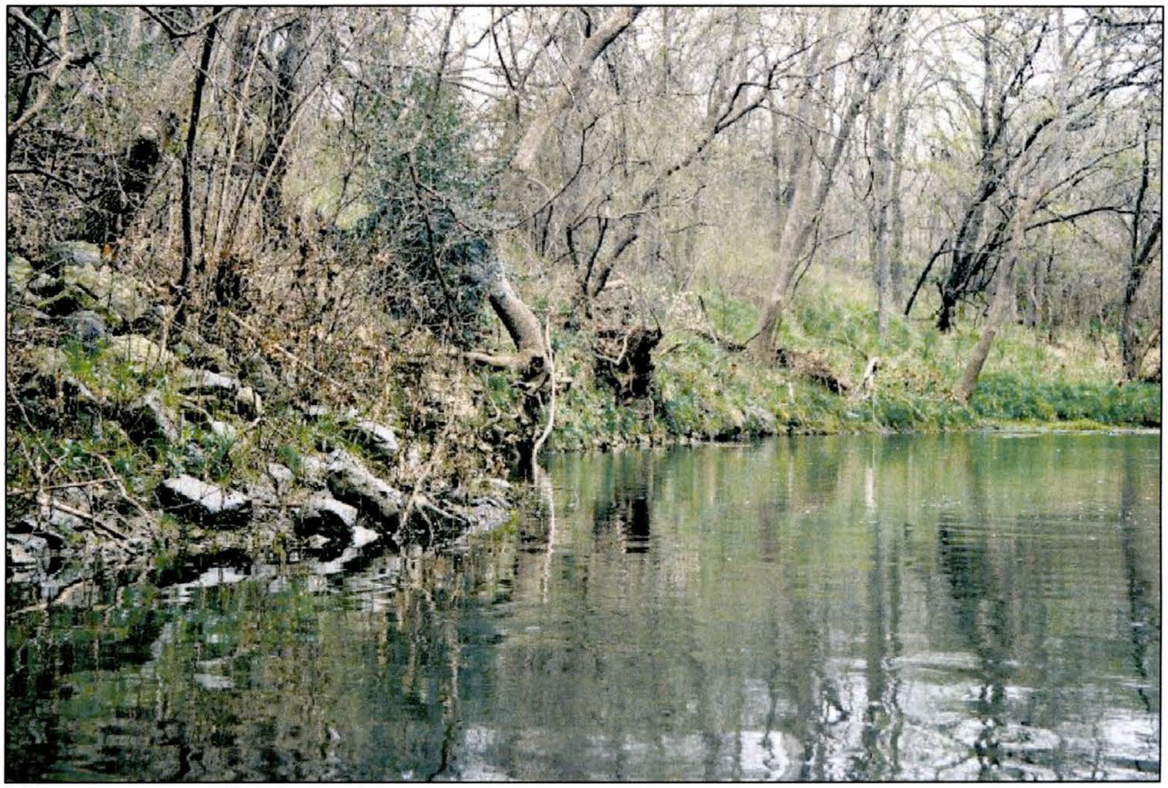

View upstream of right bank

	Low	Medium	High
Slope[1]	0.0022	0.0022	0.0022
XS Area[2]	0.2809	3.5061	10.0440
D_{max}[2]	0.4663	0.7437	1.1765
Velocity[2]	0.1158	0.2286	0.7010
Radius[3]	0.0415	0.3554	0.5632
d_{84}[1]	0.0892	0.0892	0.0892
w-to-d[3]	14.3791	13.1148	15.0259
$n_{observed}$	0.0488	0.1035	0.0459
Bathurst	0.0880	0.0364	0.0341
Cowan	0.0380	0.0380	0.0380
Jarrett	0.0919	0.0652	0.0605
Limerinos	0.1339	0.0402	0.0372
USGS	0.0350	0.0350	0.0350

08144500 San Saba River at Menard, TX
30.9189°N, 99.7853°W

View downstream of left bank

	Low	Medium	High
Slope[1]	0.0009	0.0009	0.0009
XS Area[2]	0.4845	2.7528	10.5090
D_{max}[2]	0.9876	1.0546	1.3716
Velocity[2]	0.2530	0.2073	0.2286
Radius[3]	0.1288	0.2759	0.4818
d_{84}[1]	0.0847	0.0847	0.0847
w-to-d[3]	3.2407	9.2486	15.7778
$n_{observed}$	0.0304	0.0616	0.0811
Bathurst	0.0451	0.0374	0.0343
Cowan	0.0540	0.0540	0.0540
Jarrett	0.0576	0.0510	0.0466
Limerinos	0.0526	0.0417	0.0374
USGS	0.0380	0.0380	0.0380

08147000 Colorado River near San Saba, TX
31.2178°N, 98.5642°W

	Low	Medium	High
Slope[1]	0 0005	0 0005	0.0005
XS Area[2]	2 6226	9.3930	35.3400
D_{max}[2]	0.5913	0.7010	1.0698
Velocity[2]	0.4023	0 3566	0.7285
Radius[3]	0.1161	0 2905	0.5174
d_{84}[1]	n/a	n/a	n/a
w-to-d[3]	38 1443	46.0870	63.8177
$n_{observed}$	0.0129	0.0268	0.0193
Bathurst	n/a	n/a	n/a
Cowan	n/a	n/a	n/a
Jarrett	0 0476	0 0411	0.0375
Limerinos	n/a	n/a	n/a
USGS	n/a	n/a	n/a

08148500 North Llano River near Junction, TX
30.5183°N, 99.8108°W

View downstream

	Low	Medium	High
Slope[1]	0.0018	0.0018	0.0018
XS Area[2]	0.2930	2.5761	6.6495
D_{max}[2]	2.3165	2.4018	2.5573
Velocity[2]	0.3719	0.2408	0.6218
Radius[3]	0.0552	0.2944	0.2110
d_{84}[1]	0.0780	0.0780	0.0780
w-to-d[3]	1.1184	3.0457	12.1573
$n_{observed}$	0.0166	0.0784	0.0243
Bathurst	0.0624	0.0360	0.0383
Cowan	0.0400	0.0400	0.0400
Jarrett	0.0823	0.0630	0.0664
Limerinos	0.0810	0.0398	0.0430
USGS	0.0410	0.0410	0.0410

08150000 Llano River near Junction, TX
30.5042°N, 99.7342°W

	Low	Medium	High
Slope[1]	0 0024	0 0024	0.0024
XS Area[2]	7.6167	8.9094	30.5040
D_{max}[2]	1.3320	1.3746	1 4722
Velocity[2]	0.4907	0 3170	0 2256
Radius[3]	0 3105	0.4897	0 7449
d_{84}[1]	n/a	n/a	n/a
w-to-d[3]	18.3066	13.0820	27 7433
$n_{observed}$	0.0460	0 0965	0 1794
Bathurst	n/a	n/a	n/a
Cowan	n/a	n/a	n/a
Jarrett	0 0685	0.0636	0.0595
Limerinos	n/a	n/a	n/a
USGS	n/a	n/a	n/a

08152900 Pedernales River near Fredericksburg, TX
30.2203°N, 98.8694°W

View upstream

	Low	Medium	High
Slope[1]	0.0024	0.0024	0.0024
XS Area[2]	1.1718	2.2785	30.9690
D_{max}[2]	1.6002	1.7221	2.1366
Velocity[2]	0.1981	0.5578	0.3536
Radius[3]	0.1702	0.2818	0.5566
d_{84}[1]	0.0724	0.0724	0.0724
w-to-d[3]	3.8095	4.2478	25.9629
$n_{observed}$	0.0752	0.0374	0.0928
Bathurst	0.0391	0.0353	0.0323
Cowan	0.0580	0.0580	0.0580
Jarrett	0.0746	0.0689	0.0618
Limerinos	0.0442	0.0391	0.0349
USGS	0.0440	0.0440	0.0440

08153500 Pedernales River near Johnson City, TX
30.2917°N, 98.3992°W

	Low	Medium	High
Slope[1]	0 0008	0.0008	0 0008
XS Area[2]	1.3206	20.5530	209.2500
D_{max}[2]	3.1425	3 2431	3.6576
Velocity[2]	0 1737	0 3018	0.2865
Radius[3]	0 1261	0.4310	1 5440
d_{84}[1]	n/a	n/a	n/a
w-to-d[3]	2 6673	14.5677	37 0000
$n_{observed}$	0 0418	0.0546	0 1346
Bathurst	n/a	n/a	n/a
Cowan	n/a	n/a	n/a
Jarrett	0 0562	0.0462	0.0376
Limerinos	n/a	n/a	n/a
USGS	n/a	n/a	n/a

08154700 Bull Creek at Loop 360 near Austin, TX
30.3719°N, 97.7844°W

View upstream of left bank

	Low	Medium	High
Slope[1]	0.0053	0.0053	0.0053
XS Area[2]	0.2539	1.2555	18.9720
D_{max}[2]	0.8047	0.9388	1.4234
Velocity[2]	0.2499	0.7193	0.5060
Radius[3]	0.0861	0.2209	0.4966
d_{84}[1]	0.0583	0.0583	0.0583
w-to-d[3]	3.0682	5.7143	26.7666
$n_{observed}$	0.0570	0.0371	0.0905
Bathurst	0.0428	0.0342	0.0308
Cowan	0.1120	0.1120	0.1120
Jarrett	0.1082	0.0930	0.0817
Limerinos	0.0500	0.0379	0.0333
USGS	0.0270	0.0270	0.0270

08155200 Barton Creek at State Highway 71 near Oak Hill, TX
30.2961°N, 97.9253°W

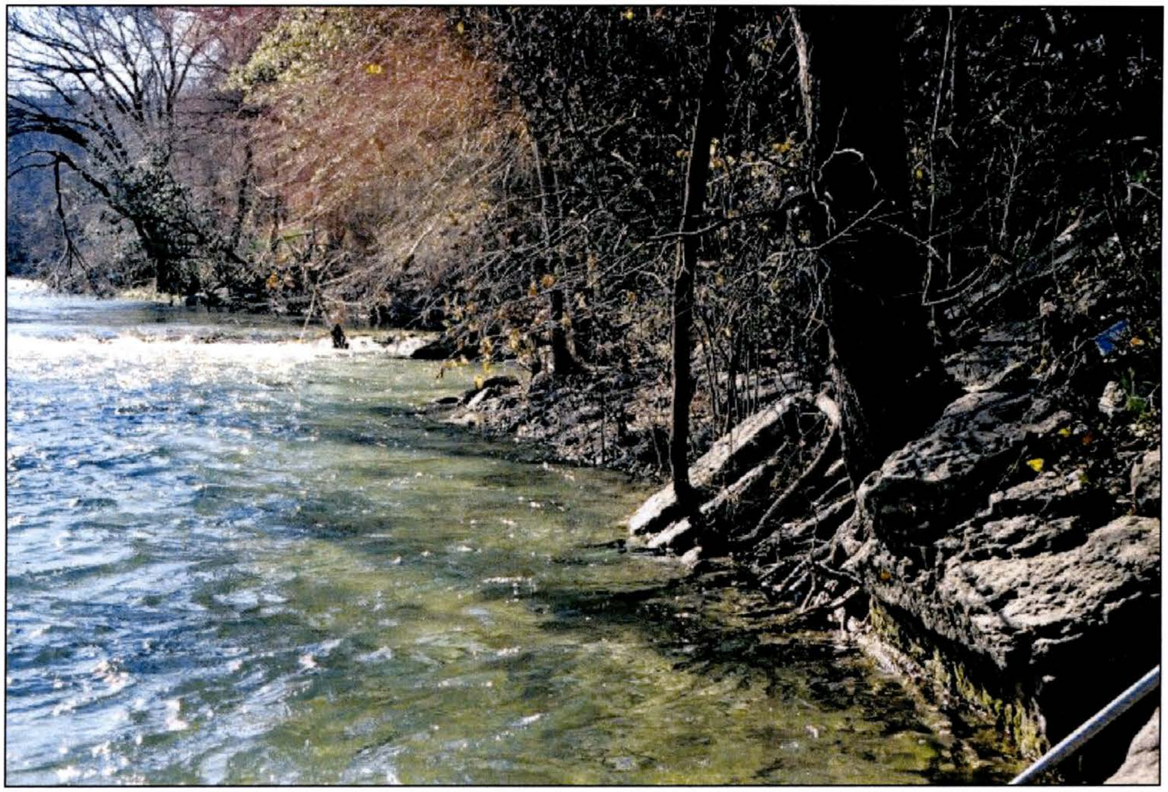

View upstream of left bank

	Low	Medium	High
Slope[1]	0.0024	0.0024	0.0024
XS Area[2]	0.3385	1.9902	12.5550
D_{max}[2]	0.7772	1.0180	1.4112
Velocity[2]	0.1341	0.7864	1.2283
Radius[3]	0.0989	0.2621	0.8908
d_{84}[1]	0.0920	0.0920	0.0920
w-to-d[3]	3.9216	7.1856	9.7192
$n_{observed}$	0.0774	0.0253	0.0366
Bathurst	0.0520	0.0390	0.0328
Cowan	0.0390	0.0390	0.0390
Jarrett	0.0814	0.0697	0.0573
Limerinos	0.0627	0.0436	0.0354
USGS	0.0430	0.0430	0.0430

08155240 Barton Creek at Lost Creek Boulevard near Austin, TX
30.2739°N, 97.8444°W

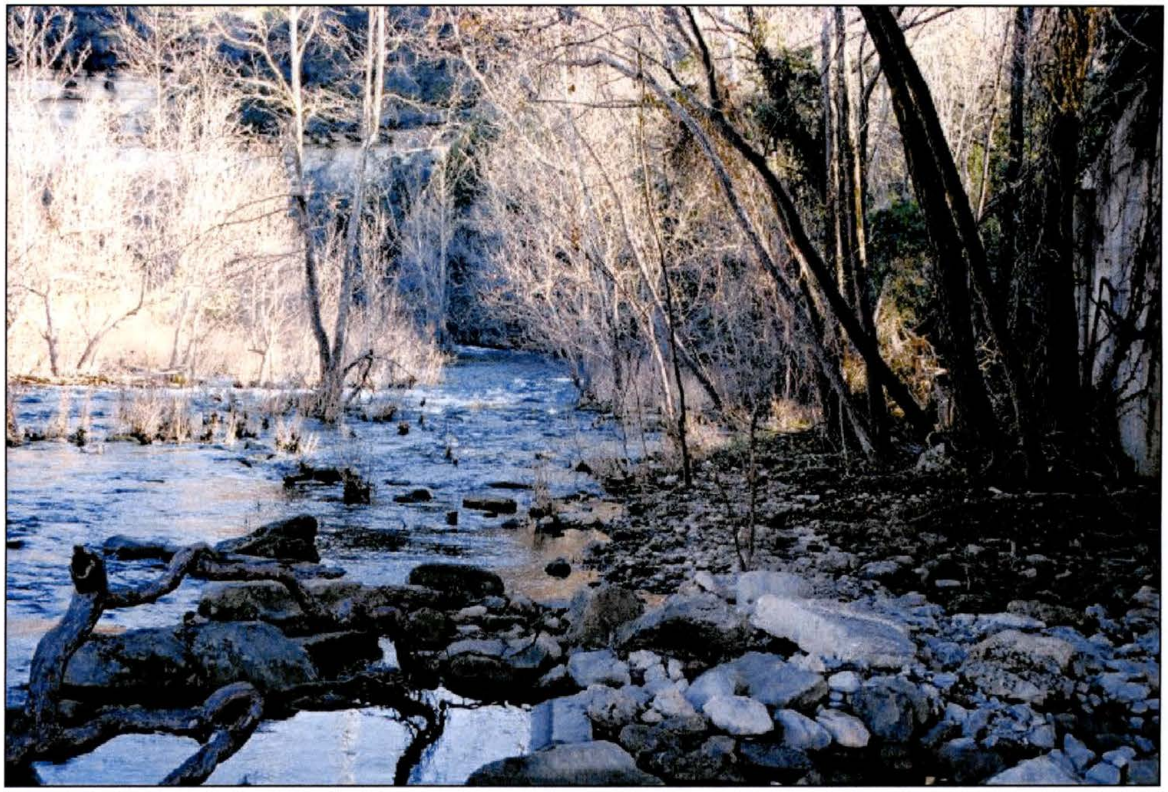

View downstream of right bank

	Low	Medium	High
Slope[1]	0.0020	0.0020	0.0020
XS Area[2]	0.2437	5.7288	24.5520
D_{max}[2]	0.5761	0.9174	1.4448
Velocity[2]	0.3018	0.3780	0.9815
Radius[3]	0.1275	0.4646	0.5582
d_{84}[1]	0.1699	0.1699	0.1699
w-to-d[3]	2.6455	13.2890	30.3797
$n_{observed}$	0.0376	0.0710	0.0309
Bathurst	0.0686	0.0435	0.0420
Cowan	0.1580	0.1580	0.1580
Jarrett	0.0742	0.0603	0.0586
Limerinos	0.0879	0.0488	0.0467
USGS	0.0650	0.0650	0.0650

08155300 Barton Creek at Loop 360 in Austin, TX
30.2444°N, 97.8019°W

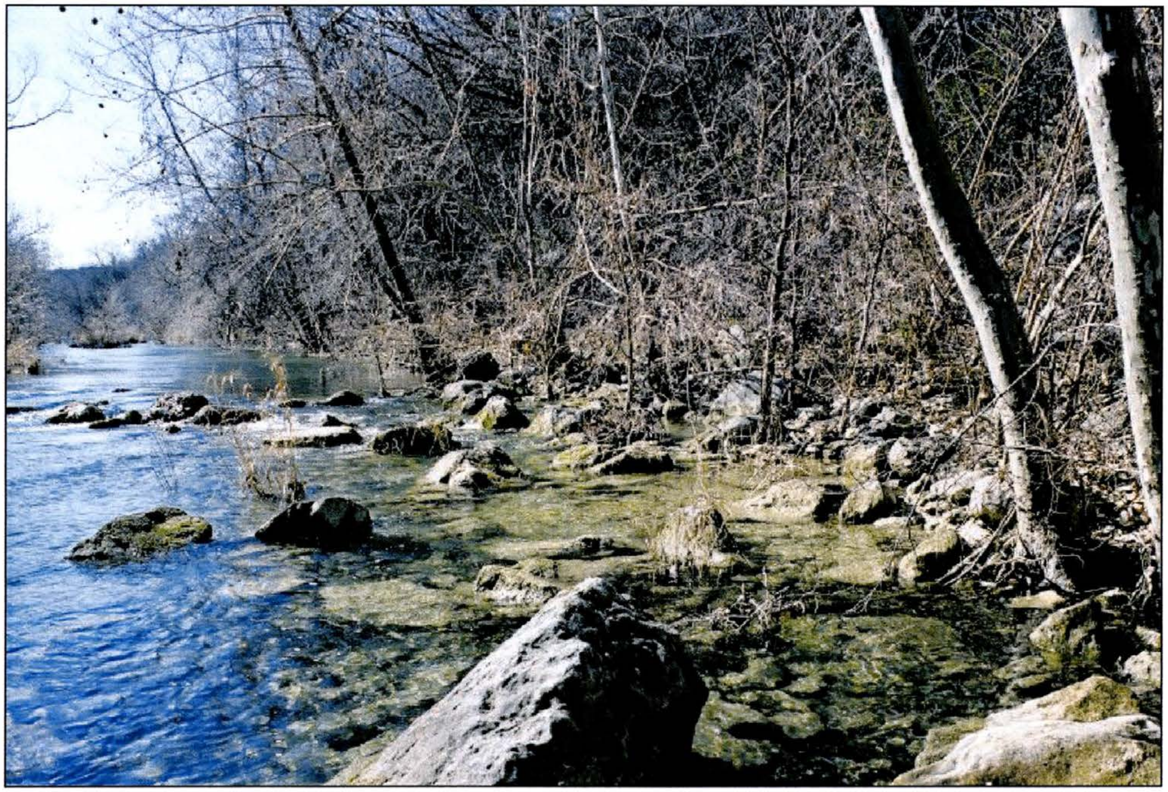

View upstream of left bank

	Low	Medium	High
Slope[1]	0.0029	0.0029	0.0029
XS Area[2]	0.9486	3.4038	10.9740
D_{max}[2]	0.8230	0.9693	1.3625
Velocity[2]	0.1402	0.2987	0.8138
Radius[3]	0.1656	0.1914	0.5102
d_{84}[1]	0.1781	0.1781	0.1781
w-to-d[3]	6.6667	18.2390	15.6600
$n_{observed}$	0.1150	0.0594	0.0419
Bathurst	0.0619	0.0580	0.0435
Cowan	0.0420	0.0420	0.0420
Jarrett	0.0798	0.0780	0.0666
Limerinos	0.0762	0.0701	0.0486
USGS	0.0320	0.0320	0.0320

08156800 Shoal Creek at West 12th Street in Austin, TX
30.2764°N, 97.7500°W

View upstream

	Low	Medium	High
Slope[1]	0.0057	0.0057	0.0057
XS Area[2]	0.7105	1.8228	15.4380
D_{max}[2]	0.5486	0.5944	1.6337
Velocity[2]	0.1006	0.5700	1.5210
Radius[3]	0.1069	0.2677	0.8516
d_{84}[1]	0.0958	0.0958	0.0958
w-to-d[3]	11.9444	11.2821	10.9142
$n_{observed}$	0.1693	0.0551	0.0447
Bathurst	0.0515	0.0394	0.0333
Cowan	0.0330	0.0330	0.0330
Jarrett	0.1068	0.0922	0.0766
Limerinos	0.0619	0.0441	0.0359
USGS	0.0300	0.0300	0.0300

08158000 Colorado River at Austin, TX
30.2444°N, 97.6942°W

View upstream of left bank

	Low	Medium	High
Slope[1]	0.0003	0.0003	0.0003
XS Area[2]	6.5751	22.2270	155.3100
D_{max}[2]	0.3993	0.6005	1.6459
Velocity[2]	0.1250	0.2926	0.3932
Radius[3]	0.2356	0.4673	1.5403
d_{84}[1]	0.0339	0.0339	0.0339
w-to-d[3]	69.8473	79.1878	59.2593
$n_{observed}$	0.0540	0.0364	0.0600
Bathurst	0.0287	0.0270	0.0258
Cowan	0.0620	0.0371	0.0333
Jarrett	0.0371	0.0333	0.0275
Limerinos	0.0312	0.0289	0.0271
USGS	0.0590	0.0590	0.0590

08158700 Onion Creek near Driftwood, TX
30.0828°N, 98.0075°W

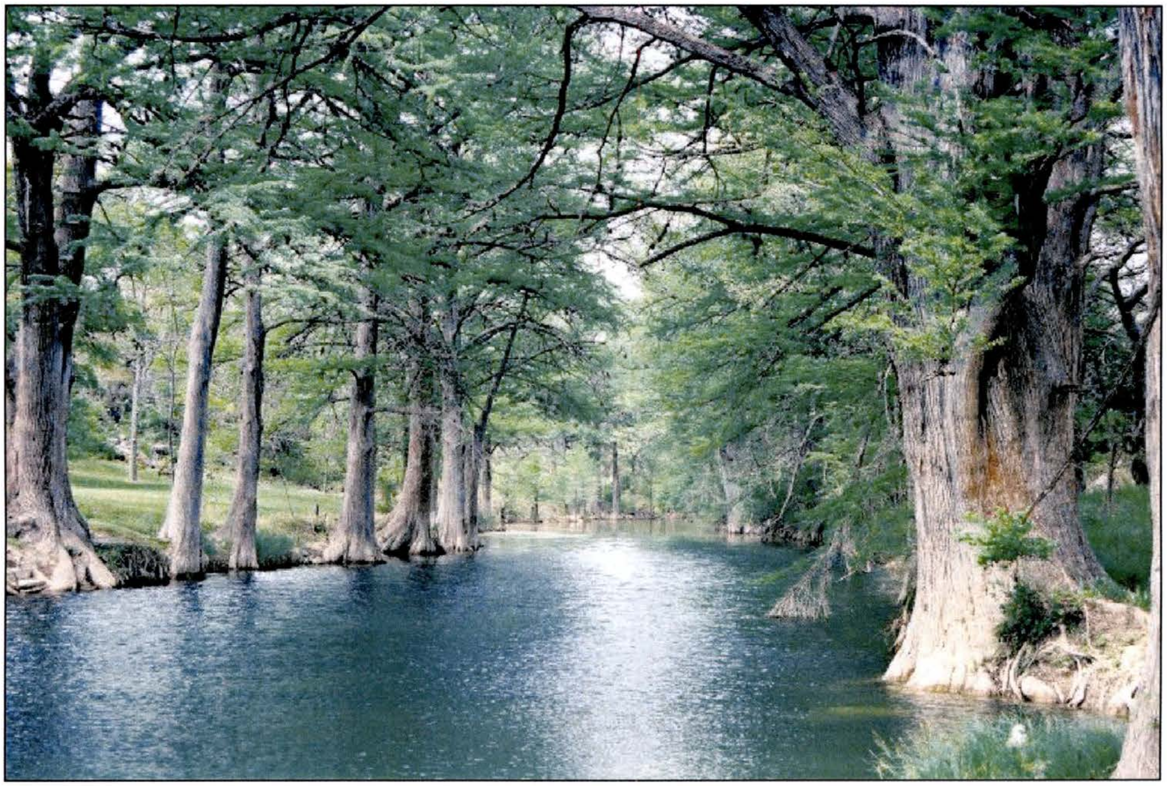

View upstream

	Low	Medium	High
Slope[1]	0.0021	0.0021	0.0021
XS Area[2]	0.8900	1.0509	11.0670
D_{max}[2]	0.3597	0.6584	1.0546
Velocity[2]	0.1128	0.8870	0.7620
Radius[3]	0.1382	0.2250	0.4466
d_{84}[1]	0.1910	0.1910	0.1910
w-to-d[3]	17.7966	6.8056	23.4104
$n_{observed}$	0.1087	0.0191	0.0352
Bathurst	0.0715	0.0566	0.0460
Cowan	0.0333	0.0333	0.0333
Jarrett	0.0745	0.0689	0.0617
Limerinos	0.0923	0.0676	0.0520
USGS	0.0360	0.0360	0.0360

08158810 Bear Creek below FM 1826 near Driftwood, TX
30.1553°N, 97.9397°W

View downstream

	Low	Medium	High
Slope[1]	0.0040	0.0040	0.0040
XS Area[2]	0.3822	2.1297	4.2873
D_{max}[2]	0.7620	0.9510	1.0241
Velocity[2]	0.3078	0.4389	0.3810
Radius[3]	0.1140	0.2818	0.6292
d_{84}[1]	0.0552	0.0552	0.0552
w-to-d[3]	3.9200	7.6923	6.2500
$n_{observed}$	0.0483	0.0619	0.1219
Bathurst	0.0385	0.0324	0.0297
Cowan	0.1010	0.1010	0.1010
Jarrett	0.0943	0.0816	0.0718
Limerinos	0.0439	0.0355	0.0319
USGS	0.0430	0.0430	0.0430

08158840 Slaughter Creek at FM 1826 near Austin, TX
30.2089°N, 97.9031°W

	Low	Medium	High
Slope[1]	0 0040	0 0040	0.0040
XS Area[2]	0 1488	2.1204	5.9148
D_{max}[2]	1 3442	1 4326	1 5758
Velocity[2]	0 4999	0.1798	0.5547
Radius[3]	0 0500	0.1673	0.3040
d_{84}[1]	n/a	n/a	n/a
w-to-d[3]	0 9524	8.6170	12 1857
$n_{observed}$	0 0172	0.1068	0.0515
Bathurst	n/a	n/a	n/a
Cowan	n/a	n/a	n/a
Jarrett	0 1076	0 0887	0.0806
Limerinos	n/a	n/a	n/a
USGS	n/a	n/a	n/a

08158922 Williamson Creek at Brush Country Boulevard, Oak Hill, TX
30.2261°N, 97.8411°W

View upstream

	Low	Medium	High
Slope[1]	0.0067	0.0067	0.0067
XS Area[2]	0.0093	1.2834	6.4170
D_{max}[2]	0.6035	0.8534	1.0272
Velocity[2]	0.2134	0.5913	0.4542
Radius[3]	0.0076	0.1972	0.3173
d_{84}[1]	0.1682	0.1682	0.1682
w-to-d[3]	0.3788	7.3571	19.5846
$n_{observed}$	0.0148	0.0468	0.0836
Bathurst	-0.0396	0.0555	0.0475
Cowan	0.1850	0.1850	0.1850
Jarrett	0.1714	0.1017	0.0943
Limerinos	-0.0326	0.0663	0.0545
USGS	0.0650	0.0650	0.0650

08158930 Williamson Creek at Manchaca Road, Austin, TX
30.2211°N, 97.7933°W

	Low	Medium	High
Slope[1]	0 0031	0.0031	0.0031
XS Area[2]	0.0800	1 1532	16.5540
D_{max}[2]	0.8016	1.0272	1.6977
Velocity[2]	0.1585	0.6980	0.7590
Radius[3]	0.0472	0.2664	0.6724
d_{84}[1]	n/a	n/a	n/a
w-to-d[3]	0.6844	3.7092	14.3627
$n_{observed}$	0 0457	0.0329	0.0561
Bathurst	n/a	n/a	n/a
Cowan	n/a	n/a	n/a
Jarrett	0 0999	0.0757	0 0653
Limerinos	n/a	n/a	n/a
USGS	n/a	n/a	n/a

08165300 North Fork Guadalupe River near Hunt, TX
30.0639°N, 99.3867°W

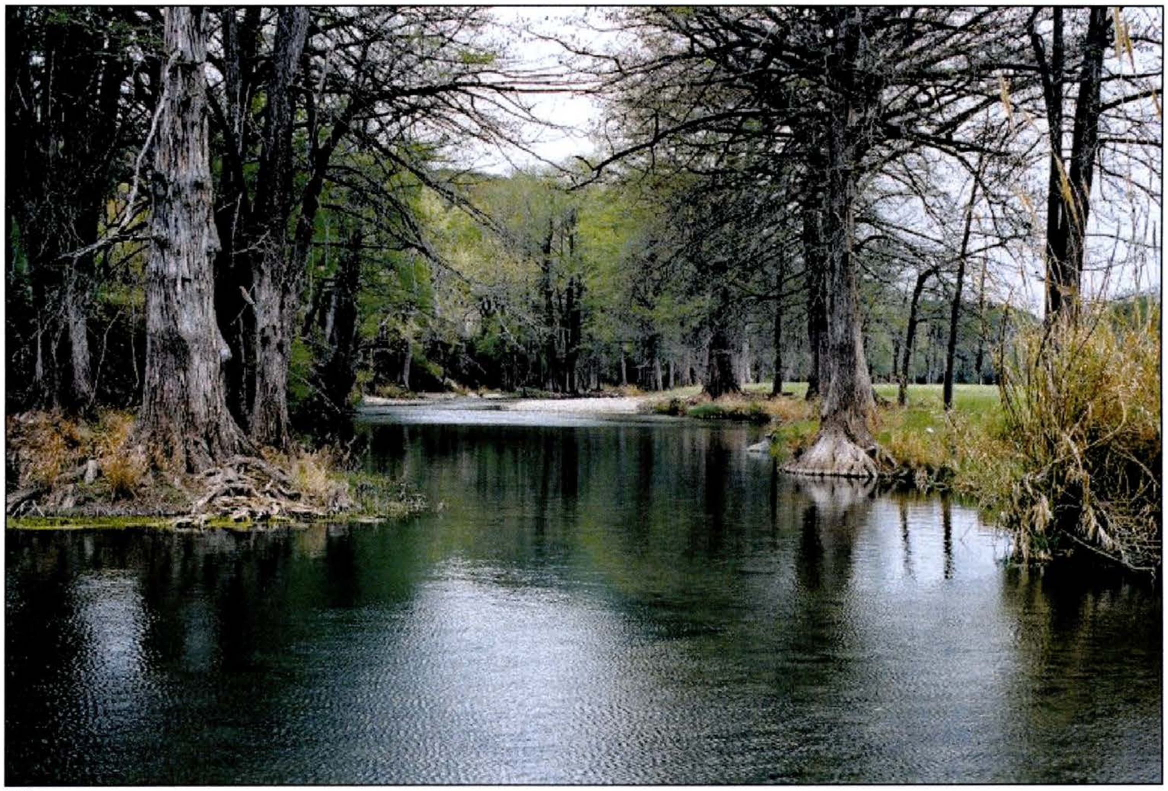

View upstream

	Low	Medium	High
Slope[1]	0.0021	0.0021	0.0021
XS Area[2]	3.1806	4.3617	4.9662
D_{max}[2]	0.4633	0.6584	0.3810
Velocity[2]	0.2164	0.2530	0.3993
Radius[3]	0.2734	0.3647	0.3926
d_{84}[1]	0.0762	0.0762	0.0762
w-to-d[3]	25.0000	18.0556	31.2000
$n_{observed}$	0.0893	0.0926	0.0616
Bathurst	0.0361	0.0345	0.0341
Cowan	0.0350	0.0350	0.0350
Jarrett	0.0668	0.0638	0.0630
Limerinos	0.0401	0.0379	0.0374
USGS	0.0320	0.0320	0.0320

08165500 Guadalupe River at Hunt, TX
30.0697°N, 99.3214°W

	Low	Medium	High
Slope[1]	0.0021	0 0021	0.0021
XS Area[2]	2.4831	3 8316	5.6079
D_{max}[2]	2.3896	2.4232	2.4994
Velocity[2]	0 5243	0.5364	0.7132
Radius[3]	0.1780	0.2583	0.3316
d_{84}[1]	n/a	n/a	n/a
w-to-d[3]	5 4847	5.7862	6 4634
$n_{observed}$	0.0277	0.0347	0.0308
Bathurst	n/a	n/a	n/a
Cowan	n/a	n/a	n/a
Jarrett	0 0715	0.0674	0.0647
Limerinos	n/a	n/a	n/a
USGS	n/a	n/a	n/a

08166000 Johnson Creek near Ingram, TX
30.1000°N, 99.2828°W

View downstream of left bank

	Low	Medium	High
Slope[1]	0.0035	0.0035	0.0035
XS Area[2]	2.2692	2.9946	10.4160
D_{max}[2]	0.1585	0.1737	0.3627
Velocity[2]	0.2621	0.3200	0.1250
Radius[3]	0.1283	0.1184	0.2712
d_{84}[1]	0.0437	0.0437	0.0437
w-to-d[3]	111.5385	145.6140	105.8824
$n_{observed}$	0.0572	0.0444	0.1977
Bathurst	0.0342	0.0348	0.0304
Cowan	0.0430	0.0430	0.0430
Jarrett	0.0885	0.0897	0.0785
Limerinos	0.0382	0.0390	0.0331
USGS	0.0320	0.0320	0.0320

08166140 Guadalupe River above Bear Creek at Kerrville, TX
30.0694°N, 99.1950°W

View downstream of right bank

	Low	Medium	High
Slope[1]	0.0021	0.0021	0.0021
XS Area[2]	8.3979	9.1698	11.1600
D_{max}[2]	0.8992	0.9967	1.1308
Velocity[2]	0.2438	0.4359	0.5243
Radius[3]	0.1873	0.1891	0.2360
d_{84}[1]	0.0272	0.0272	0.0272
w-to-d[3]	49.8305	48.6239	41.7790
$n_{observed}$	0.0616	0.0347	0.0334
Bathurst	0.0277	0.0277	0.0271
Cowan	0.0390	0.0390	0.0390
Jarrett	0.0709	0.0708	0.0684
Limerinos	0.0301	0.0301	0.0292
USGS	0.0430	0.0430	0.0430

08166200 Guadalupe River at Kerrville, TX
30.0531°N, 99.1631°W

View downstream

	Low	Medium	High
Slope[1]	0.0020	0.0020	0.0020
XS Area[2]	5.8218	9.6720	14.4150
D_{max}[2]	0.4999	0.5547	0.6431
Velocity[2]	0.2560	0.3048	0.4724
Radius[3]	0.1123	0.1611	0.2376
d_{84}[1]	0.1274	0.1274	0.1274
w-to-d[3]	103.6585	108.2418	94.3128
$n_{observed}$	0.0407	0.0434	0.0363
Bathurst	0.0600	0.0515	0.0455
Cowan	0.0370	0.0370	0.0370
Jarrett	0.0757	0.0715	0.0672
Limerinos	0.0746	0.0610	0.0522
USGS	0.0330	0.0330	0.0330

08167000 Guadalupe River at Comfort, TX
29.9694°N, 98.8925°W

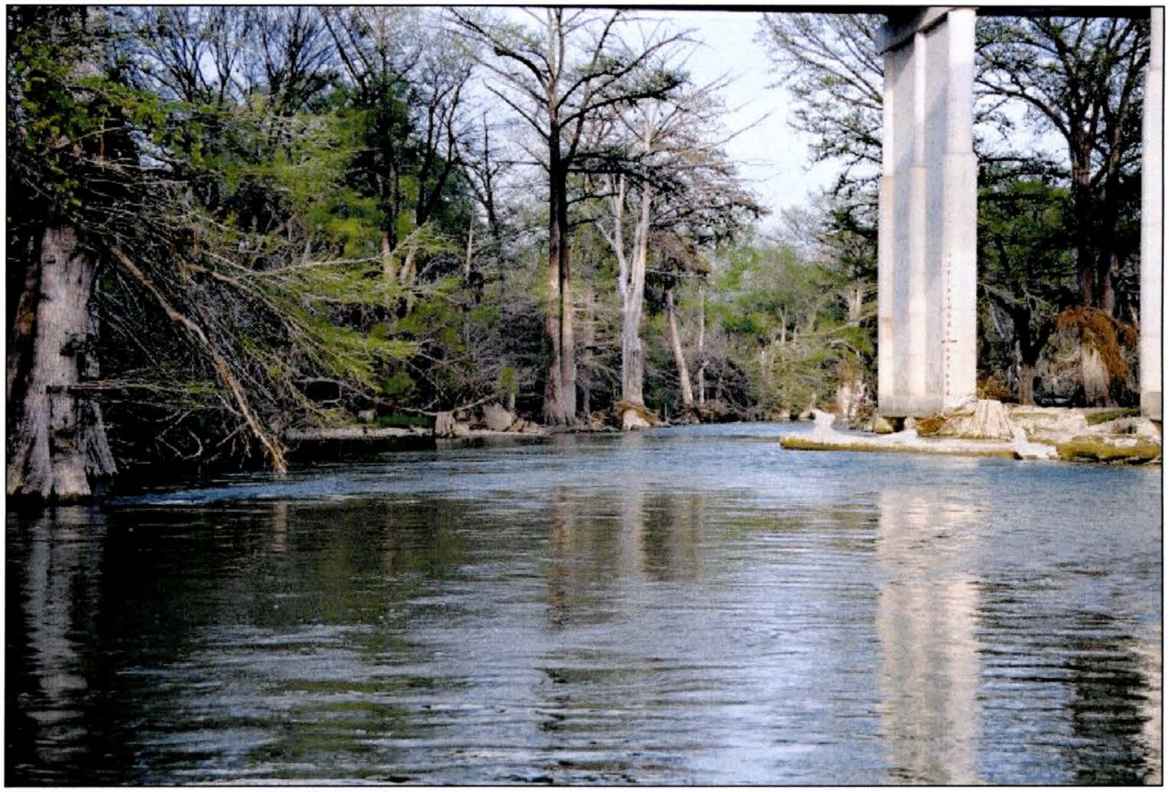

View downstream of left bank

	Low	Medium	High
Slope[1]	0.0021	0.0021	0.0021
XS Area[2]	3.6642	5.7381	17.9490
D_{max}[2]	0.3688	0.6309	0.8809
Velocity[2]	0.3810	0.7010	0.5669
Radius[3]	0.3213	0.5046	0.6749
d_{84}[1]	0.0591	0.0591	0.0591
w-to-d[3]	28.9256	17.8744	30.1038
$n_{observed}$	0.0565	0.0415	0.0623
Bathurst	0.0325	0.0309	0.0301
Cowan	0.0510	0.0510	0.0510
Jarrett	0.0651	0.0605	0.0578
Limerinos	0.0355	0.0333	0.0323
USGS	0.0450	0.0450	0.0450

08167500 Guadalupe River near Spring Branch, TX
29.8603°N, 98.3833°W

View downstream

	Low	Medium	High
Slope[1]	0.0014	0.0014	0.0014
XS Area[2]	5.3103	11.9040	23.0640
D_{max}[2]	0.6706	0.9479	1.3503
Velocity[2]	0.3597	0.5761	0.9662
Radius[3]	0.3770	0.4991	0.9958
d_{84}[1]	<0.0001	<0.0001	<0.0001
w-to-d[3]	20.9091	25.0804	16.9977
$n_{observed}$	0.0548	0.0413	0.0390
Bathurst	0.0085	0.0087	0.0093
Cowan	0.0360	0.0360	0.0360
Jarrett	0.0560	0.0536	0.0480
Limerinos	0.0086	0.0088	0.0094
USGS	0.0320	0.0320	0.0320

08167800 Guadalupe River at Sattler, TX
29.8589°N, 98.1797°W

	Low	Medium	High
Slope[1]	0.0017	0.0017	0.0017
XS Area[2]	4 6035	10.6020	72.7260
D_{max}[2]	1 3655	1.4996	1.8837
Velocity[2]	0.7376	0.6431	0.4145
Radius[3]	0.3093	0.4787	1.5458
d_{84}[1]	n/a	n/a	n/a
w-to-d[3]	10 7143	14.6341	22 9773
$n_{observed}$	0.0259	0.0397	0.1345
Bathurst	n/a	n/a	n/a
Cowan	n/a	n/a	n/a
Jarrett	0 0616	0.0574	0.0476
Limerinos	n/a	n/a	n/a
USGS	n/a	n/a	n/a

08168500 Guadalupe River above Comal River at New Braunfels, TX
29.7147°N, 98.1097°W

View downstream

	Low	Medium	High
Slope[1]	0.0008	0.0008	0.0008
XS Area[2]	17.9490	24.5520	40.9200
D_{max}[2]	0.6218	0.7559	1.0363
Velocity[2]	0.2408	0.4694	0.8504
Radius[3]	0.5604	0.7461	1.3898
d_{84}[1]	0.0447	0.0447	0.0447
w-to-d[3]	49.5098	41.5323	26.4118
$n_{observed}$	0.0815	0.0506	0.0423
Bathurst	0.0285	0.0280	0.0272
Cowan	0.0330	0.0330	0.0330
Jarrett	0.0443	0.0423	0.0383
Limerinos	0.0305	0.0298	0.0288
USGS	0.0380	0.0380	0.0380

08169000 Comal River at New Braunfels, TX
29.7058°N, 98.1222°W

	Low	Medium	High
Slope[1]	0.0012	0.0012	0.0012
XS Area[2]	17 2050	17 2980	21.3900
D_{max}[2]	1 3167	1 3411	1.4143
Velocity[2]	0.5304	0 5761	0.6187
Radius[3]	0.6243	0.6417	0.7843
d_{84}[1]	n/a	n/a	n/a
w-to-d[3]	20 8333	20.0000	19 1810
$n_{observed}$	0.0472	0.0443	0.0471
Bathurst	n/a	n/a	n/a
Cowan	n/a	n/a	n/a
Jarrett	0 0486	0 0484	0 0468
Limerinos	n/a	n/a	n/a
USGS	n/a	n/a	n/a

08170500 San Marcos River at San Marcos, TX
29.8889°N, 97.9339°W

	Low	Medium	High
Slope[1]	0 0022	0 0022	0 0022
XS Area[2]	10 2300	10 0440	12.3690
D_{max}[2]	1 6673	1 7678	1 7526
Velocity[2]	0.5547	0.7590	0.7864
Radius[3]	0 5459	0 5966	0 6486
d_{84}[1]	n/a	n/a	n/a
w-to-d[3]	11.0603	9 3103	10.6957
$n_{observed}$	0.0568	0 0440	0 0449
Bathurst	n/a	n/a	n/a
Cowan	n/a	n/a	n/a
Jarrett	0.0608	0.0600	0 0592
Limerinos	n/a	n/a	n/a
USGS	n/a	n/a	n/a

08171000 Blanco River at Wimberley, TX
29.9942°N, 98.0886°W


View upstream of left bank

	Low	Medium	High
Slope[1]	0.0019	0.0019	0.0019
XS Area[2]	8.7141	12.1830	15.6240
D_{max}[2]	1.1125	1.2466	1.3899
Velocity[2]	0.1372	0.3109	0.5334
Radius[3]	0.2283	0.3092	0.4190
d_{84}[1]	0.0439	0.0439	0.0439
w-to-d[3]	34.2466	31.5403	26.7544
$n_{observed}$	0.1189	0.0642	0.0458
Bathurst	0.0311	0.0300	0.0291
Cowan	0.0380	0.0380	0.0380
Jarrett	0.0666	0.0634	0.0604
Limerinos	0.0340	0.0325	0.0313
USGS	0.0430	0.0430	0.0430

08171300 Blanco River near Kyle, TX
29.9792°N, 97.9097°W

	Low	Medium	High
Slope[1]	0 0011	0.0011	0.0011
XS Area[2]	2.3064	9 5790	12 5550
D_{max}[2]	1 4600	1 5453	1.8136
Velocity[2]	0.3566	0 2042	0.6005
Radius[3]	0.2031	0.3629	0 4971
d_{84}[1]	n/a	n/a	n/a
w-to-d[3]	7 5157	16 9625	13.7815
$n_{observed}$	0 0314	0.0808	0 0339
Bathurst	n/a	n/a	n/a
Cowan	n/a	n/a	n/a
Jarrett	0 0561	0.0511	0.0486
Limerinos	n/a	n/a	n/a
USGS	n/a	n/a	n/a

08177700 Olmos Creek at Dresden Drive, San Antonio, TX
29.4989°N, 98.5100°W

	Low	Medium	High
Slope[1]	0 0029	0.0029	0 0029
XS Area[2]	0.0893	0.3720	0.7496
D_{max}[2]	0.5578	0 6157	0.7407
Velocity[2]	0 1097	0 6462	1 1064
Radius[3]	0.0263	0 1067	0.1900
d_{84}[1]	n/a	n/a	n/a
w-to-d[3]	5.7377	5 2970	4 9383
$n_{observed}$	0 0431	0.0186	0.0160
Bathurst	n/a	n/a	n/a
Cowan	n/a	n/a	n/a
Jarrett	0.1071	0 0856	0 0781
Limerinos	n/a	n/a	n/a
USGS	n/a	n/a	n/a

08178700 Salado Creek at Loop 410 at San Antonio, TX
29.5158°N, 98.4308°W

View upstream

	Low	Medium	High
Slope[1]	0.0011	0.0011	0.0011
XS Area[2]	0.0688	1.1160	2.3064
D_{max}[2]	0.7803	0.9327	1.0424
Velocity[2]	0.0732	0.5486	0.9693
Radius[3]	0.0316	0.1751	0.3284
d_{84}[1]	0.0933	0.0933	0.0933
w-to-d[3]	1.9531	6.5359	6.4327
$n_{observed}$	0.0455	0.0190	0.0164
Bathurst	0.1324	0.0431	0.0375
Cowan	0.0540	0.0540	0.0540
Jarrett	0.0769	0.0585	0.0529
Limerinos	0.2901	0.0494	0.0416
USGS	0.0320	0.0320	0.0320

08178880 Medina River at Bandera, TX
29.7236°N, 99.0697°W

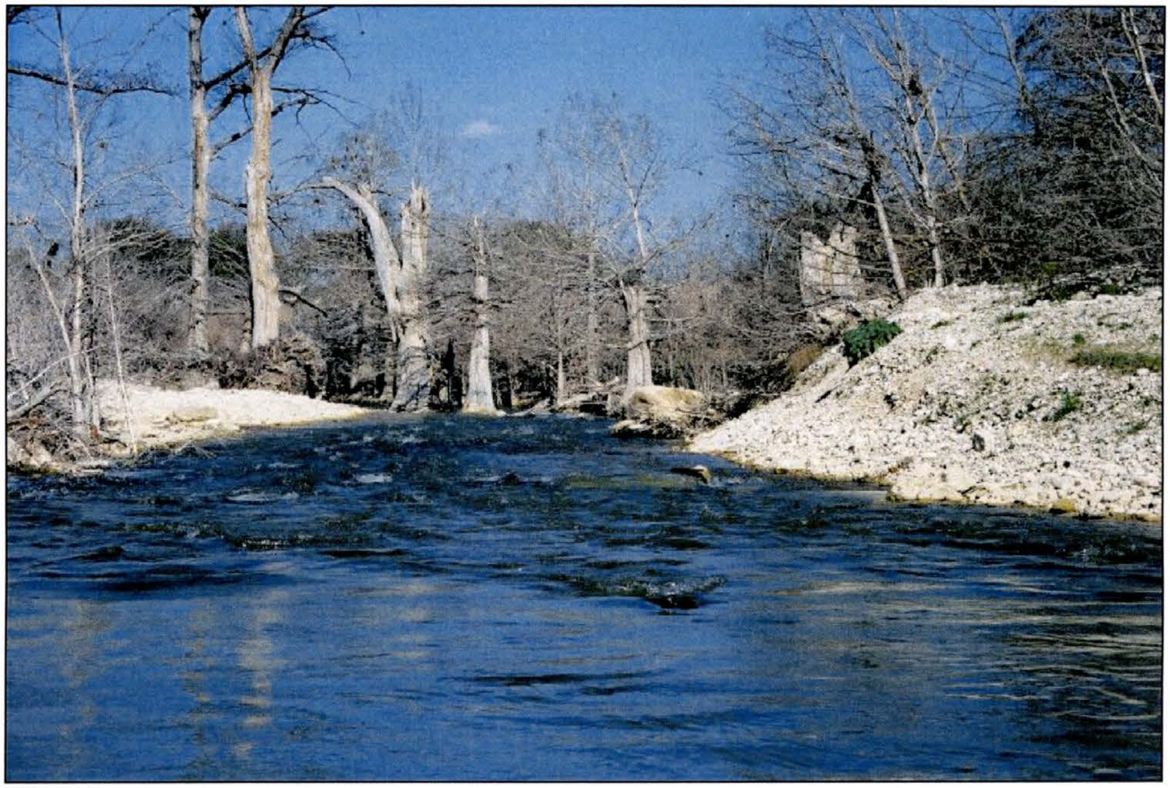

View downstream

	Low	Medium	High
Slope[1]	0.0022	0.0022	0.0022
XS Area[2]	1.6275	9.0303	13.2060
D_{max}[2]	1.0698	1.7343	1.7191
Velocity[2]	0.2408	0.4694	0.7193
Radius[3]	0.1813	0.4775	0.6667
d_{84}[1]	0.1265	0.1265	0.1265
w-to-d[3]	8.1481	10.7206	11.3475
$n_{observed}$	0.0627	0.0613	0.0500
Bathurst	0.0492	0.0390	0.0371
Cowan	0.0350	0.0350	0.0350
Jarrett	0.0726	0.0621	0.0589
Limerinos	0.0576	0.0431	0.0405
USGS	0.0260	0.0260	0.0260

08180500 USGS Medina River near Riomedina, TX
29.4981°N, 98.9044°W

	Low	Medium	High
Slope[1]	0.0017	0.0017	0.0017
XS Area[2]	3.5898	8.9745	11.3460
D_{max}[2]	0 3353	0 4084	0.6126
Velocity[2]	0.2804	0.2713	0 4084
Radius[3]	0.2901	0.4195	0.5089
d_{84}[1]	n/a	n/a	n/a
w-to-d[3]	34 9091	50.3731	36 3184
$n_{observed}$	0.0638	0.0843	0.0637
Bathurst	n/a	n/a	n/a
Cowan	n/a	n/a	n/a
Jarrett	0 0614	0 0579	0 0561
Limerinos	n/a	n/a	n/a
USGS	n/a	n/a	n/a

08181400 Helotes Creek at Helotes, TX
29.5783°N, 98.6914°W

View downstream of right bank

	Low	Medium	High
Slope[1]	0.0050	0.0050	0.0050
XS Area[2]	0.2074	1.4229	0.8686
D_{max}[2]	0.4755	0.5243	0.5212
Velocity[2]	0.2316	0.1158	0.3780
Radius[3]	0.1498	0.2194	0.1339
d_{84}[1]	<0.0001	<0.0001	<0.0001
w-to-d[3]	2.1154	12.2093	12.2807
$n_{observed}$	0.0861	0.2221	0.0490
Bathurst	0.0078	0.0081	0.0077
Cowan	0.0640	0.0640	0.0640
Jarrett	0.0970	0.0912	0.0987
Limerinos	0.0080	0.0082	0.0079
USGS	0.0430	0.0430	0.0430

08183850 Cibolo Creek at IH 10 above Boerne, TX
29.8144°N, 98.7533°W

View downstream of left bank

	Low	Medium	High
Slope[1]	0.0036	0.0036	0.0036
XS Area[2]	0.3199	0.4752	1.1625
D_{max}[2]	0.3749	0.3962	0.4481
Velocity[2]	0.2225	0.3109	0.5913
Radius[3]	0.0418	0.0597	0.1355
d_{84}[1]	<0.0001	<0.0001	<0.0001
w-to-d[3]	20.3252	20.0000	19.0476
$n_{observed}$	0.0326	0.0296	0.0269
Bathurst	0.0083	0.0085	0.0090
Cowan	0.0280	0.0280	0.0280
Jarrett	0.1074	0.1015	0.0890
Limerinos	0.0085	0.0087	0.0092
USGS	0.0270	0.0270	0.0270

08185000 Cibolo Creek at Selma, TX
29.5939°N, 98.3108°W

View downstream of left bank

	Low	Medium	High
Slope[1]	0.0023	0.0023	0.0023
XS Area[2]	1.0044	26.1330	35.6190
D_{max}[2]	0.8138	1.0516	1.3716
Velocity[2]	0.0396	0.0427	0.3018
Radius[3]	0.1755	0.8848	1.5581
d_{84}[1]	0.0055	0.0055	0.0055
w-to-d[3]	6.7416	26.0870	14.6667
$n_{observed}$	0.3782	1.0326	0.2129
Bathurst	0.0192	0.0191	0.0193
Cowan	0.0310	0.0310	0.0310
Jarrett	0.0736	0.0568	0.0519
Limerinos	0.0202	0.0198	0.0200
USGS	0.0510	0.0510	0.0510

08190000 Nueces River at Laguna, TX
29.4283°N, 99.9969°W

View downstream

	Low	Medium	High
Slope[1]	0.0026	0.0026	0.0026
XS Area[2]	1.9158	3.4131	8.1840
D_{max}[2]	1.0272	0.9388	1.0577
Velocity[2]	0.7163	0.6005	0.8961
Radius[3]	0.2654	0.2348	0.4558
d_{84}[1]	0.1886	0.1886	0.1886
w-to-d[3]	6.7359	15.3571	16.8588
$n_{observed}$	0.0293	0.0322	0.0336
Bathurst	0.0529	0.0553	0.0455
Cowan	0.0340	0.0340	0.0340
Jarrett	0.0716	0.0730	0.0657
Limerinos	0.0621	0.0656	0.0514
USGS	0.0430	0.0430	0.0430

08190500 West Nueces River near Brackettville, TX
29.4725°N, 100.2361°W

View upstream

	Low	Medium	High
Slope[1]	0.0027	0.0027	0.0027
XS Area[2]	0.2483	0.7208	2.3343
D_{max}[2]	0.4084	0.4359	0.6218
Velocity[2]	0.0853	0.1554	0.3627
Radius[3]	0.0490	0.1020	0.2269
d_{84}[1]	0.0794	0.0794	0.0794
w-to-d[3]	12.2388	16.0839	16.4216
$n_{observed}$	0.0811	0.0725	0.0530
Bathurst	0.0684	0.0473	0.0380
Cowan	0.0320	0.0320	0.0320
Jarrett	0.0948	0.0843	0.0742
Limerinos	0.0921	0.0560	0.0425
USGS	0.0430	0.0430	0.0430

08195000 Frio River at Concan, TX
29.4883°N, 99.7044°W

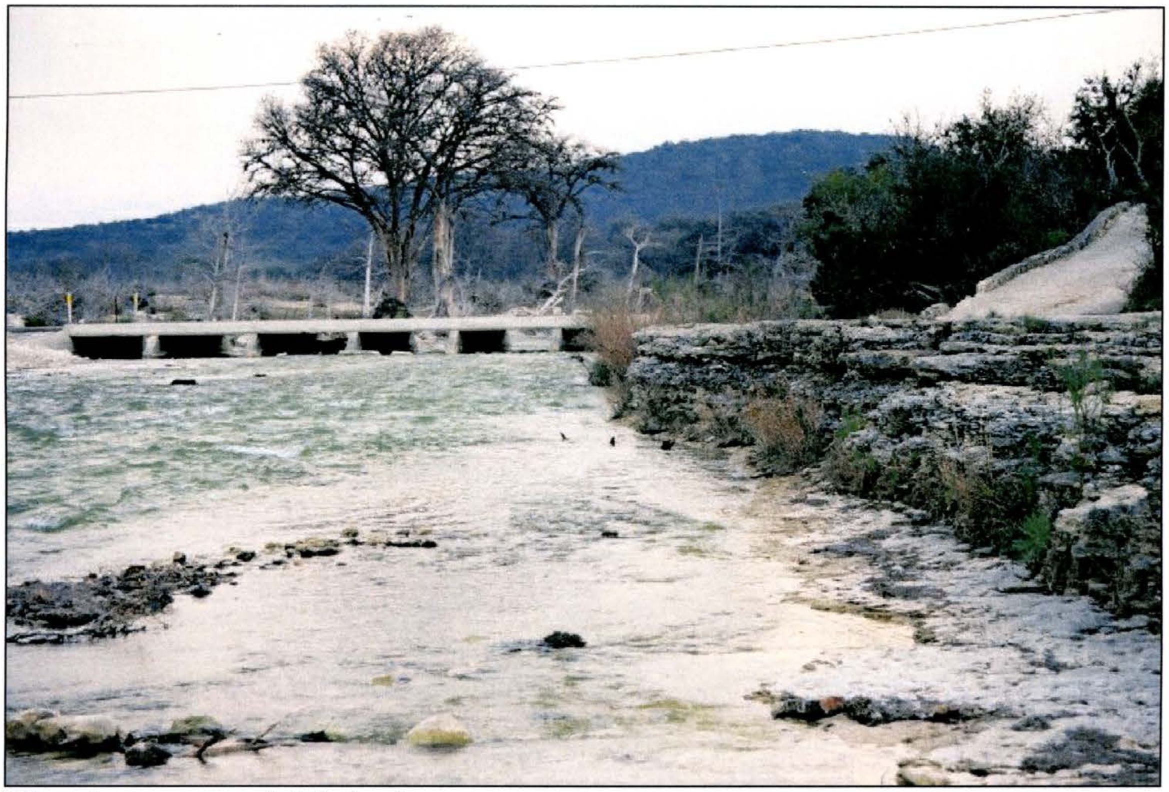

View downstream of right bank

	Low	Medium	High
Slope[1]	0.0025	0.0025	0.0025
XS Area[2]	1.7670	2.6598	5.9706
D_{max}[2]	1.0942	1.1521	1.2527
Velocity[2]	0.3139	0.5456	0.6248
Radius[3]	0.1768	0.1972	0.2760
d_{84}[1]	0.0840	0.0840	0.0840
w-to-d[3]	8.9136	11.5344	17.1533
$n_{observed}$	0.0502	0.0310	0.0339
Bathurst	0.0411	0.0400	0.0373
Cowan	0.0310	0.0310	0.0310
Jarrett	0.0757	0.0743	0.0704
Limerinos	0.0468	0.0453	0.0415
USGS	0.0430	0.0430	0.0430

08196000 Dry Frio River near Reagan Wells, TX
29.5044°N, 99.7811°W

View upstream

	Low	Medium	High
Slope[1]	0.0032	0.0032	0.0032
XS Area[2]	0.6724	1.1997	7.3656
D_{max}[2]	0.5547	0.6370	0.7254
Velocity[2]	0.1646	0.3688	0.1341
Radius[3]	0.1085	0.1279	0.2773
d_{84}[1]	0.1138	0.1138	0.1138
w-to-d[3]	10.9890	14.5933	36.5546
$n_{observed}$	0.0782	0.0389	0.1794
Bathurst	0.0567	0.0529	0.0418
Cowan	0.0280	0.0280	0.0280
Jarrett	0.0885	0.0862	0.0762
Limerinos	0.0696	0.0635	0.0471
USGS	0.0280	0.0280	0.0280

08198000 Sabinal River near Sabinal, TX
29.4908°N, 99.4925°W

View downstream

	Low	Medium	High
Slope[1]	0.0025	0.0025	0.0025
XS Area[2]	1.8228	4.5198	4.2873
D_{max}[2]	1.4691	1.5484	1.6093
Velocity[2]	0.2774	0.3200	0.5547
Radius[3]	0.2121	0.3320	0.4037
d_{84}[1]	0.0699	0.0699	0.0699
w-to-d[3]	5.4979	8.5630	6.2879
$n_{observed}$	0.0641	0.0749	0.0492
Bathurst	0.0367	0.0341	0.0332
Cowan	0.0320	0.0320	0.0320
Jarrett	0.0735	0.0684	0.0663
Limerinos	0.0410	0.0374	0.0362
USGS	0.0300	0.0300	0.0300

08200000 Hondo Creek near Tarpley, TX
29.5694°N, 99.2464°W

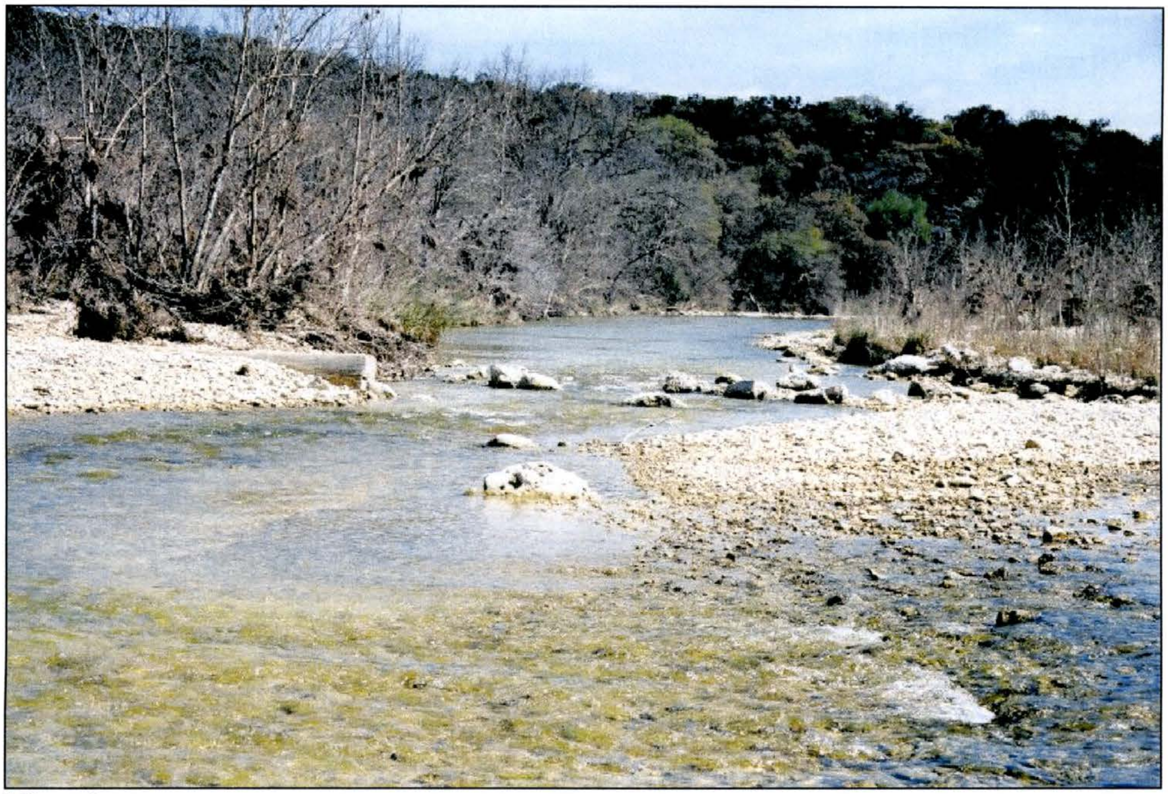

View downstream

	Low	Medium	High
Slope[1]	0.0033	0.0033	0.0033
XS Area[2]	0.7533	1.3671	5.7753
D_{max}[2]	0.0701	0.1341	0.2957
Velocity[2]	0.1006	0.5425	0.4023
Radius[3]	0.0894	0.1927	0.3579
d_{84}[1]	0.0688	0.0688	0.0688
w-to-d[3]	118.2609	50.9091	52.5773
$n_{observed}$	0.1147	0.0355	0.0723
Bathurst	0.0460	0.0372	0.0335
Cowan	0.0450	0.0450	0.0450
Jarrett	0.0925	0.0818	0.0741
Limerinos	0.0544	0.0417	0.0367
USGS	0.0320	0.0320	0.0320

08201500 Seco Creek at Miller Ranch near Utopia, TX
29.5731°N, 99.4028°W

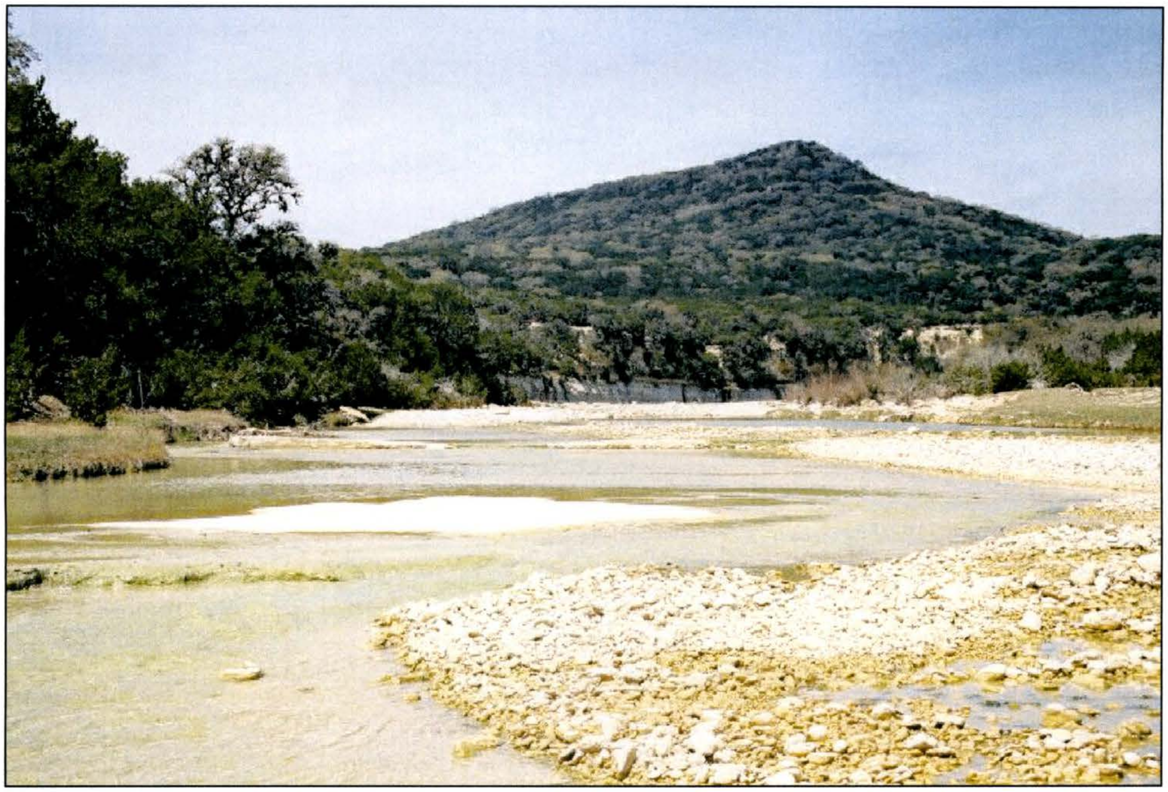

View upstream

	Low	Medium	High
Slope[1]	0.0020	0.0020	0.0020
XS Area[2]	0.2306	1.1904	1.1997
D_{max}[2]	0.3932	0.4724	0.5791
Velocity[2]	0.1158	0.1494	0.5517
Radius[3]	0.0989	0.1041	0.1498
d_{84}[1]	0.0216	0.0216	0.0216
w-to-d[3]	5.5814	24.1290	13.6842
$n_{observed}$	0.0826	0.0662	0.0229
Bathurst	0.0282	0.0279	0.0267
Cowan	0.0320	0.0320	0.0320
Jarrett	0.0773	0.0767	0.0723
Limerinos	0.0309	0.0307	0.0289
USGS	0.0270	0.0270	0.0270

APPENDIX II

ALL RESEARCH DATA

Appendix II represents all collected data used in this research study. The data are arranged by variable with subscript L, M, and H indicating the level of flow represented. Those variables without a subscript remained constant for all flow levels. Abbreviated variable names represent the following: A=cross-sectional area; W=channel width; D_{max}=maximum depth; V=velocity; P=wetted perimeter; R=hydraulic radius; d_{84}=84th percentile of sediment size; n_{obs}=observed roughness; B=roughness calculated using Bathurst's equation; J=Jarrett's roughness value; and L=Limerinos' roughness value.

Site #	Site Name	Lat	Lon	A_L
08101000	Cowhouse Ck at Pidcoke, TX	31 285	-97 885	0 387
08103800	Lampasas Rv nr Kempner, TX	31 082	-98 016	1 972
08103900	S Fk Rocky Ck nr Briggs, TX	30 911	-98 037	0 353
08104100	Lampasas Rv nr Belton, TX	31 002	-97 492	1 153
08104700	N Fk San Gabriel Rv nr Georgetown, TX	30 662	-97 711	0 949
08104900	S Fk San Gabriel Rv at Georgetown, TX	30 626	-97 691	0 187
08105100	Berry Ck nr Georgetown, TX	30.691	-97.656	0 281
08144500	San Saba Rv at Menard, TX	30 919	-99.785	0 485
08147000	Colorado Rv nr San Saba, TX	31 218	-98.564	2 623
08148500	N Llano Rv nr Junction, TX	30 518	-99.811	0.293
08150000	Llano Rv nr Junction, TX	30.504	-99 734	7 617
08152900	Pedernales Rv nr Fredericksburg, TX	30.220	-98.869	1 172
08153500	Pedernales Rv nr Johnson City, TX	30.292	-98 399	1 321
08154700	Bull Ck at Loop 360 nr Austin, TX	30.372	-97.784	0 254
08155200	Barton Ck at SH 71 nr Oak Hill, TX	30 296	-97 925	0 339
08155240	Barton Ck at Lost Ck Blvd nr Austin, TX	30 274	-97 844	0.244
08155300	Barton Ck at Loop 360, Austin, TX	30 244	-97 802	0 949
08156800	Shoal Ck at W 12th St, Austin, TX	30.276	-97.750	0 711
08158000	Colorado Rv at Austin, TX	30 244	-97 694	6.575
08158700	Onion Ck nr Driftwood, TX	30 083	-98 008	0 890
08158810	Bear Ck bl FM 1826 nr Driftwood, TX	30 155	-97 940	0 382
08158840	Slaughter Ck at FM 1826 nr Austin, TX	30 209	-97 903	0 149
08158922	Williamson Ck at Brush Country Blvd, Oak Hill, TX	30 226	-97 841	0 009
08158930	Williamson Ck at Manchaca Rd, Austin, TX	30 221	-97.793	0 080
08165300	N Fk Guadalupe Rv nr Hunt, TX	30 064	-99 387	3 181
08165500	Guadalupe Rv at Hunt, TX	30 070	-99.321	2.483
08166000	Johnson Ck nr Ingram, TX	30.100	-99.283	2 269
08166140	Guadalupe Rv abv Bear Ck at Kerrville, TX	30 069	-99 195	8 398
08166200	Guadalupe Rv at Kerrville, TX	30 053	-99.163	5 822
08167000	Guadalupe Rv at Comfort, TX	29.969	-98 893	3 664
08167500	Guadalupe Rv nr Spring Branch, TX	29 860	-98 383	5 310
08167800	Guadalupe Rv at Sattler, TX	29 859	-98 180	4 604
08168500	Guadalupe Rv abv Comal Rv at New Braunfels, TX	29 715	-98 110	17.949
08169000	Comal Rv at New Braunfels, TX	29 706	-98 122	17 205
08170500	San Marcos Rv at San Marcos, TX	29.889	-97.934	10.230
08171000	Blanco Rv at Wimberley, TX	29 994	-98.089	8 714
08171300	Blanco Rv nr Kyle, TX	29 979	-97 910	2 306
08177700	Olmos Ck at Dresden Dr, San Antonio, TX	29.499	-98.510	0 089
08178700	Salado Ck at Loop 410 at San Antonio, TX	29 516	-98.431	0 069
08178880	Medina Rv at Bandera, TX	29 724	-99 070	1.628
08180500	USGS Medina Rv nr Riomedina, TX	29 498	-98 904	3 590
08181400	Helotes Ck at Helotes, TX	29 578	-98 691	0 207
08183850	Cibolo Ck at IH 10 abv Boerne, TX	29 814	-98 753	0.320
08185000	Cibolo Ck at Selma, TX	29 594	-98 311	1 004
08190000	Nueces Rv at Laguna, TX	29 428	-99.997	1.916
08190500	W Nueces Rv nr Brackettville, TX	29 473	-100.236	0 248
08195000	Frio Rv at Concan, TX	29 488	-99 704	1 767
08196000	Dry Frio Rv nr Reagan Wells, TX	29 504	-99 781	0 672
08198000	Sabinal Rv nr Sabinal, TX	29 491	-99.493	1 823
08200000	Hondo Ck nr Tarpley, TX	29 569	-99.246	0 753
08201500	Seco Ck at Miller Ranch nr Utopia, TX	29 573	-99 403	0.231

Site #	A_M	A_H	W_L	W_M	W_H	D_{max-L}	D_{max-M}	D_{max-H}	V_L	V_M
08101000	1.544	11 439	4.267	7.315	24.994	0.927	1 076	1.515	0.207	0 902
08103800	4.836	14.043	16.307	20 117	25.146	1.103	1 183	1.457	0.317	0 539
08103900	2.334	11.439	4.267	8.230	11 887	0.408	0.664	0.957	0.213	0.475
08104100	8.779	46.686	9.357	22.555	34.138	1.548	1.875	3.018	0.320	0.439
08104700	4 213	21.483	3.962	11 278	25.603	1.417	1.664	2.042	0.207	0.311
08104900	2.995	22.134	2 560	10.058	24.994	0.750	0.954	1.564	0.354	0 485
08105100	3.506	10.044	6.706	9.754	17.678	0.466	0.744	1 177	0.116	0 229
08144500	2.753	10.509	3 200	9 754	21.641	0 988	1.055	1 372	0.253	0.207
08147000	9.393	35.340	22.555	32 309	68 275	0 591	0.701	1.070	0.402	0 357
08148500	2 576	6.650	2.591	7 315	31 090	2 316	2.402	2.557	0.372	0.241
08150000	8.909	30.504	24.384	17 983	40 843	1 332	1.375	1.472	0.491	0.317
08152900	2.279	30.969	6 096	7 315	55 474	1 600	1.722	2.137	0.198	0 558
08153500	20 553	209.250	8.382	47.244	135.331	3.142	3.243	3.658	0.174	0.302
08154700	1 256	18 972	2.469	5.364	38.100	0.805	0 939	1.423	0.250	0.719
08155200	1.990	12.555	3 048	7 315	13 716	0.777	1.018	1.411	0.134	0.786
08155240	5 729	24.552	1 524	12.192	43 891	0 576	0.917	1.445	0.302	0 378
08155300	3.404	10.974	5 486	17.678	21.336	0.823	0.969	1.362	0.140	0 299
08156800	1.823	15.438	6.553	6.706	17.831	0.549	0.594	1.634	0.101	0 570
08158000	22.227	155.310	27.889	47 549	97.536	0.399	0.600	1.646	0.125	0.293
08158700	1.051	11.067	6.401	4.481	24 689	0.360	0.658	1.055	0 113	0.887
08158810	2.130	4.287	2.987	7.315	6.401	0.762	0.951	1.024	0 308	0.439
08158840	2 120	5.915	1.280	12.344	19.202	1.344	1.433	1 576	0.500	0 180
08158922	1.283	6 417	0 229	6 279	20 117	0.604	0.853	1.027	0.213	0.591
08158930	1.153	16.554	0.549	3.810	24.384	0.802	1.027	1.698	0 158	0.698
08165300	4.362	4 966	11.582	11.887	11 887	0.463	0.658	0.381	0.216	0.253
08165500	3.832	5.608	13 106	14.021	16.154	2.390	2 423	2.499	0.524	0.536
08166000	2.995	10.416	17.678	25 298	38.405	0.158	0.174	0.363	0 262	0.320
08166140	9.170	11.160	44.806	48.463	47.244	0.899	0.997	1.131	0 244	0.436
08166200	9 672	14.415	51.816	60.046	60.655	0.500	0.555	0.643	0.256	0.305
08167000	5 738	17 949	10 668	11.278	26.518	0.369	0.631	0.881	0.381	0.701
08167500	11 904	23 064	14 021	23.774	22.951	0.671	0.948	1.350	0.360	0.576
08167800	10.602	72 726	14 630	21.946	43 282	1.366	1.500	1 884	0.738	0.643
08168500	24 552	40 920	30 785	31.394	27 371	0.622	0 756	1.036	0.241	0.469
08169000	17.298	21.390	27.432	26 822	27.127	1.317	1.341	1.414	0.530	0 576
08170500	10 044	12.369	18.440	16.459	18.745	1.667	1.768	1.753	0.555	0.759
08171000	12.183	15.624	38.100	39.319	37.186	1.113	1.247	1.390	0.137	0.311
08171300	9.579	12 555	10 973	26 213	24.994	1 460	1.545	1.814	0.357	0 204
08177700	0.372	0 750	3 200	3.261	3 658	0.558	0.616	0 741	0.110	0.646
08178700	1.116	2.306	1.524	6.096	6.706	0 780	0.933	1 042	0.073	0.549
08178880	9.030	13.206	8 717	18 593	19 507	1.070	1.734	1.719	0.241	0.469
08180500	8 975	11.346	11 704	20.574	22 250	0.335	0.408	0 613	0.280	0.271
08181400	1.423	0.869	1.006	6 401	6 401	0 475	0.524	0.521	0 232	0.116
08183850	0.475	1.163	7 620	7 925	8.534	0.375	0 396	0.448	0.223	0 311
08185000	26.133	35 619	5 486	27.432	20.117	0 814	1.052	1.372	0.040	0.043
08190000	3.413	8.184	6 919	14.417	17.831	1 027	0.939	1.058	0.716	0.600
08190500	0.721	2.334	4.999	7 010	10.211	0.408	0.436	0.622	0 085	0.155
08195000	2.660	5.971	9.754	13.289	21.488	1.094	1.152	1.253	0.314	0.546
08196000	1 200	7 366	6.096	9.296	26 518	0.555	0.637	0.725	0.165	0.369
08198000	4.520	4.287	8.077	13.259	10.119	1.469	1.548	1.609	0.277	0.320
08200000	1 367	5.775	8.291	6 828	15.545	0 070	0.134	0.296	0.101	0.543
08201500	1 190	1.200	2.195	11.400	7.925	0.393	0.472	0 579	0 116	0.149

Site #	V_H	P_L	P_M	P_H	R_L	R_M	R_H	d_{84}	n_{obs-L}	n_{obs-M}	n_{obs-H}
08101000	0.963	4 652	7.625	25.177	0 083	0 202	0.454	n/a	0.039	0.016	0 026
08103800	0 777	16.455	20.255	25.314	0 120	0.239	0.555	n/a	0 036	0.034	0.041
08103900	0 524	4 345	8.336	13.801	0.081	0.280	0.829	n/a	0.059	0.060	0.113
08104100	0.735	9.856	22.865	34 667	0 117	0.384	1 347	n/a	0.036	0 058	0.079
08104700	0.338	4 872	11 759	25 927	0.195	0 358	0 829	0.041	0.094	0 094	0.151
08104900	0.738	2.967	10 238	25 188	0.063	0.293	0.879	0.093	0.020	0.041	0.056
08105100	0.701	6.770	9.866	17.834	0.041	0.355	0.563	0.089	0.049	0.103	0.046
08144500	0.229	3.761	9.979	21.814	0.129	0.276	0.482	0.085	0.030	0.062	0 081
08147000	0.728	22.586	32.339	68.309	0.116	0.290	0 517	n/a	0.013	0.027	0.019
08148500	0 622	5 308	8.751	31.507	0.055	0.294	0.211	0.078	0.017	0.078	0.024
08150000	0.226	24.529	18.192	40 949	0 311	0.490	0.745	n/a	0 046	0.097	0.179
08152900	0 354	6.885	8.085	55 638	0.170	0.282	0.557	0.072	0.075	0.037	0 093
08153500	0.287	10.477	47.687	135.529	0.126	0 431	1.544	n/a	0.042	0.055	0.135
08154700	0.506	2 947	5 684	38.206	0.086	0.221	0 497	0.058	0.057	0 037	0.091
08155200	1.228	3.422	7.593	14.094	0 099	0.262	0.891	0 092	0.077	0.025	0 037
08155240	0.981	1.911	12 329	43 986	0.128	0.465	0.558	0.170	0.038	0.071	0.031
08155300	0 814	5.728	17.784	21.509	0.166	0.191	0.510	0.178	0.115	0.059	0.042
08156800	1.521	6.644	6.810	18.128	0.107	0.268	0 852	0.096	0.169	0.055	0.045
08158000	0 393	27 904	47.569	100.828	0.236	0.467	1 540	0.034	0 054	0.036	0.060
08158700	0.762	6.441	4 670	24.779	0 138	0.225	0.447	0.191	0.109	0.019	0.035
08158810	0 381	3 353	7.558	6.814	0.114	0.282	0.629	0.055	0.048	0.062	0.122
08158840	0.555	2.978	12.673	19.459	0.050	0 167	0.304	n/a	0.017	0.107	0 052
08158922	0 454	1.228	6 507	20.221	0 008	0.197	0.317	0.168	0.015	0.047	0.084
08158930	0 759	1 695	4 329	24.619	0 047	0 266	0.672	n/a	0 046	0.033	0.056
08165300	0 399	11 632	11 960	12 649	0 273	0.365	0.393	0.076	0.089	0.093	0.062
08165500	0 713	13 951	14.835	16 910	0.178	0.258	0.332	n/a	0.028	0.035	0.031
08166000	0.125	17.682	25.302	38 414	0 128	0.118	0.271	0.044	0.057	0 044	0.198
08166140	0.524	44.842	48.504	47.298	0.187	0.189	0.236	0 027	0.062	0.035	0 033
08166200	0.472	51.826	60.056	60.669	0.112	0.161	0.238	0.127	0.041	0.043	0.036
08167000	0 567	11.406	11.371	26.595	0.321	0.505	0.675	0.059	0.056	0.041	0.062
08167500	0.966	14 085	23 850	23.162	0 377	0.499	0.996	0.000	0.055	0.041	0.039
08167800	0 415	14.883	22.150	47.049	0.309	0.479	1.546	n/a	0.026	0 040	0.134
08168500	0.850	32.028	32.906	29.444	0.560	0.746	1.390	0.045	0.081	0.051	0.042
08169000	0.619	27 558	26.956	27.274	0.624	0 642	0.784	n/a	0.047	0.044	0.047
08170500	0 786	18 739	16.835	19.070	0.546	0 597	0 649	n/a	0 057	0.044	0.045
08171000	0.533	38.165	39.398	37.289	0.228	0.309	0 419	0 044	0.119	0.064	0 046
08171300	0.600	11.355	26 394	25.255	0 203	0 363	0.497	n/a	0 031	0.081	0.034
08177700	1.106	3.389	3.486	3 946	0 026	0.107	0 190	n/a	0.043	0 019	0.016
08178700	0.969	2.181	6 375	7.022	0 032	0.175	0.328	0.093	0 045	0.019	0.016
08178880	0.719	8.976	18 914	19.808	0 181	0 477	0.667	0.127	0.063	0 061	0 050
08180500	0 408	12.375	21.391	22 295	0.290	0.420	0.509	n/a	0.064	0 084	0.064
08181400	0.378	1.384	6.486	6.485	0 150	0.219	0.134	0.000	0.086	0.222	0 049
08183850	0.591	7.657	7.964	8.581	0.042	0 060	0.135	0.000	0.033	0.030	0.027
08185000	0 302	5 723	29 535	22.860	0.176	0.885	1 558	0 005	0.378	1.033	0.213
08190000	0.896	7.218	14 539	17.956	0.265	0.235	0.456	0.189	0.029	0.032	0.034
08190500	0.363	5.065	7.064	10 286	0.049	0.102	0.227	0.079	0.081	0.073	0.053
08195000	0.625	9.996	13.488	21.634	0 177	0.197	0.276	0.084	0.050	0 031	0.034
08196000	0.134	6.196	9.383	26.557	0 109	0.128	0.277	0.114	0.078	0.039	0.179
08198000	0.555	8 595	13 616	10 619	0.212	0.332	0.404	0.070	0.064	0 075	0.049
08200000	0.402	8.431	7.096	16.136	0.089	0.193	0.358	0.069	0.115	0.035	0.072
08201500	0.552	2.331	11.439	8 009	0 099	0 104	0.150	0.022	0.083	0.066	0.023

Site #	B_L	B_M	B_H	Cowan	J_L	J_M	J_H	L_L	L_M	L_H	USGS
08101000	n/a	n/a	n/a	n/a	0.077	0.067	0.059	n/a	n/a	n/a	n/a
08103800	n/a	n/a	n/a	n/a	0.078	0.069	0.061	n/a	n/a	n/a	n/a
08103900	n/a	n/a	n/a	n/a	0.103	0.085	0.071	n/a	n/a	n/a	n/a
08104100	n/a	n/a	n/a	n/a	0.079	0.065	0.053	n/a	n/a	n/a	n/a
08104700	0.031	0.029	0.027	0.066	0.082	0.074	0.065	0.034	0.031	0.029	0.043
08104900	0.066	0.038	0.033	0.032	0.083	0.065	0.054	0.087	0.043	0.036	0.030
08105100	0.088	0.036	0.034	0.038	0.092	0.065	0.061	0.134	0.040	0.037	0.035
08144500	0.045	0.037	0.034	0.054	0.058	0.051	0.047	0.053	0.042	0.037	0.038
08147000	n/a	n/a	n/a	n/a	0.048	0.041	0.037	n/a	n/a	n/a	n/a
08148500	0.062	0.036	0.038	0.040	0.082	0.063	0.066	0.081	0.040	0.043	0.041
08150000	n/a	n/a	n/a	0.000	0.068	0.064	0.060	n/a	n/a	n/a	n/a
08152900	0.039	0.035	0.032	0.058	0.075	0.069	0.062	0.044	0.039	0.035	0.044
08153500	n/a	n/a	n/a	n/a	0.056	0.046	0.038	n/a	n/a	n/a	n/a
08154700	0.043	0.034	0.031	0.112	0.108	0.093	0.082	0.050	0.038	0.033	0.027
08155200	0.052	0.039	0.033	0.039	0.081	0.070	0.057	0.063	0.044	0.035	0.043
08155240	0.069	0.044	0.042	0.158	0.074	0.060	0.059	0.088	0.049	0.047	0.065
08155300	0.062	0.058	0.043	0.042	0.080	0.078	0.067	0.076	0.070	0.049	0.032
08156800	0.052	0.039	0.033	0.033	0.107	0.092	0.077	0.062	0.044	0.036	0.030
08158000	0.029	0.027	0.026	0.062	0.037	0.033	0.028	0.031	0.029	0.027	0.059
08158700	0.072	0.057	0.046	0.033	0.074	0.069	0.062	0.092	0.068	0.052	0.036
08158810	0.039	0.032	0.030	0.101	0.094	0.082	0.072	0.044	0.035	0.032	0.043
08158840	n/a	n/a	n/a	n/a	0.108	0.089	0.081	n/a	n/a	n/a	n/a
08158922	-0.040	0.056	0.048	0.185	0.171	0.102	0.094	-0.033	0.066	0.054	0.065
08158930	n/a	n/a	n/a	n/a	0.100	0.076	0.065	n/a	n/a	n/a	n/a
08165300	0.036	0.035	0.034	0.035	0.067	0.064	0.063	0.040	0.038	0.037	0.032
08165500	n/a	n/a	n/a	n/a	0.072	0.067	0.065	n/a	n/a	n/a	n/a
08166000	0.034	0.035	0.030	0.043	0.089	0.090	0.079	0.038	0.039	0.033	0.032
08166140	0.028	0.028	0.027	0.039	0.071	0.071	0.068	0.030	0.030	0.029	0.043
08166200	0.060	0.051	0.046	0.037	0.076	0.071	0.067	0.075	0.061	0.052	0.033
08167000	0.032	0.031	0.030	0.051	0.065	0.061	0.058	0.036	0.033	0.032	0.045
08167500	0.008	0.009	0.009	0.036	0.056	0.054	0.048	0.009	0.009	0.009	0.032
08167800	n/a	n/a	n/a	n/a	0.062	0.057	0.048	n/a	n/a	n/a	n/a
08168500	0.029	0.028	0.027	0.033	0.044	0.042	0.038	0.031	0.030	0.029	0.038
08169000	n/a	n/a	n/a	n/a	0.049	0.048	0.047	n/a	n/a	n/a	n/a
08170500	n/a	n/a	n/a	n/a	0.061	0.060	0.059	n/a	n/a	n/a	n/a
08171000	0.031	0.030	0.029	0.038	0.067	0.063	0.060	0.034	0.033	0.031	0.043
08171300	n/a	n/a	n/a	n/a	0.056	0.051	0.049	n/a	n/a	n/a	n/a
08177700	n/a	n/a	n/a	n/a	0.107	0.086	0.078	n/a	n/a	n/a	n/a
08178700	0.132	0.043	0.037	0.054	0.077	0.058	0.053	0.290	0.049	0.042	0.032
08178880	0.049	0.039	0.037	0.035	0.073	0.062	0.059	0.058	0.043	0.041	0.026
08180500	n/a	n/a	n/a	n/a	0.061	0.058	0.056	n/a	n/a	n/a	n/a
08181400	0.008	0.008	0.008	0.064	0.097	0.091	0.099	0.008	0.008	0.008	0.043
08183850	0.008	0.008	0.009	0.028	0.107	0.101	0.089	0.009	0.009	0.009	0.027
08185000	0.019	0.019	0.019	0.031	0.074	0.057	0.052	0.020	0.020	0.020	0.051
08190000	0.053	0.055	0.046	0.034	0.072	0.073	0.066	0.062	0.066	0.051	0.043
08190500	0.068	0.047	0.038	0.032	0.095	0.084	0.074	0.092	0.056	0.043	0.043
08195000	0.041	0.040	0.037	0.031	0.076	0.074	0.070	0.047	0.045	0.042	0.043
08196000	0.057	0.053	0.042	0.028	0.089	0.086	0.076	0.070	0.063	0.047	0.028
08198000	0.037	0.034	0.033	0.032	0.073	0.068	0.066	0.041	0.037	0.036	0.030
08200000	0.046	0.037	0.034	0.045	0.093	0.082	0.074	0.054	0.042	0.037	0.032
08201500	0.028	0.028	0.027	0.032	0.077	0.077	0.072	0.031	0.031	0.029	0.027

WORKS CITED

Arcement, George J., Jr. and Verne R. Schneider. 1989. *Guide for selecting Manning's Roughness Coefficients for natural channels and flood plains.* U. S. Geological Survey Water-Supply Paper 2339. Washington, DC: U. S. Geological Survey.

Baker, Victor R. 1975. *Flood hazards along the Balcones Escarpment in central Texas: Alternative approaches to their recognition, mapping, and management.* Circular 75-5. Austin, TX: University of Texas Bureau of Economic Geology.

Bathurst, James C. 1985. Flow resistance estimation in mountain rivers. *Journal of Hydraulic Engineering* 111, no. 4: 625-43.

_______. 1993. Flow resistance through the channel network. In *Channel Network Hydrology,* eds. Keith Beven and Michael J. Kirkby, 69-98. Chichester, England: Wiley Publishers.

_______. 2002. At-a-site variation and minimum flow resistance for mountain rivers. *Journal of Hydrology* 269: 11-26.

Barnes, Harry H., Jr. 1967. *Roughness characteristics of natural channels.* U. S. Geological Survey Water-Supply Paper 1849. Washington, DC: U. S. Geological Survey.

Bednarz, Sarah W., Richard G. Boehm, and Roger M. Downs. 1994. *Geography for life: National geography standards 1994.* Washington, DC: National Council for Geographic Education.

Benson, M. A. and Tate Dalrymple. 1967. *Techniques of water-resources investigations of the United States Geological Survey.* Washington, DC: U. S. Geological Survey.

Bray, Dale I. 1972. Generalized regime-type analysis of Alberta rivers. Ph. D. diss., University of Alberta, Edmonton, Canada.

Cowan, W. L. 1956. Estimating hydraulic roughness coefficients. *Agricultural Engineering 37*: 473-75.

Dingman, S. Lawrence and Keshav P. Sharma. 1997. Statistical development and validation of discharge equations for natural channels. *Journal of Hydrology* 199, no. 1-2: 13-35.

Earl, Richard A. and Todd H. Votteler. 2002. Major water issues facing south-central Texas. In *Water for Texas, 2000 and beyond: Proceedings of the conference in College Station, TX, September 23-24, 2000*, 2-34. College Station, TX: Texas A&M Press.

105

Fenneman, Nevin M. 1931. *Physiography of the western United States*. New York, NY: McGraw-Hill Book Company.

_______. 1938. *Physiography of the eastern United States*. New York, NY: McGraw-Hill Book Company.

Fonstad, Mark A. 2000. Spatio-temporal variation in the power of mountain streams. Ph. D. diss., Arizona State University.

Garnero, Ed. 2002. *Excel 7: Curve-fitting II: Solver* [on-line]. Tempe, AZ: Arizona State University; available from http://geology.asu.edu/~glg410/lectures/L12_Excel_curvefittingII.html; Internet. Accessed on 10 April 2003.

Goudie, Andrew, ed. 1981. *Geomorphological techniques.* London: George Allen & Unwin.

Graf, William L. and Kris Randall. 1997. *The physical integrity of streams: A guidance document for river management*. Report submitted in partial fulfillment of Arizona Department of Environmental Quality Contract 95-0137.

Hudson, J. Paul. 2000. *Goode's world atlas.* USA: Rand McNally & Company.

Jarrett, Robert D. 1984. Hydraulics of high-gradient streams. *Journal of Hydraulic Engineering* 110: 1519-39.

Knighton, David. 1998. *Fluvial forms and processes: A new perspective*. New York, NY: Oxford University Press, Inc.

Li, Zhe and Juntao Zhang. 2001. Calculation of field Manning's Roughness Coefficient. *Agricultural Water Management* 49: 153-61.

Limerinos, J. T. 1970. *Determination of the Manning Coefficient from measured bed roughness in natural channels.* U. S. Geological Survey Water-Supply Paper 1898-B. Washington, DC: U. S. Geological Survey.

Lounsbury, John F. and Frank T. Aldrich. 1986. *Introduction to geographic field methods and techniques.* Englewood Cliffs, NJ: Macmillan Publishing Company.

Manning, Robert. 1891. On the flow of water in open channels and pipes. *Transactions of the Institution of Civil Engineers* 20: 161-207.

Marcus, W. Andrew, Keith Roberts, Leslie Harvey, and Gary Tackman. 1992. An evaluation of methods for estimating Manning's *n* in small mountain streams. *Mountain Research and Development* 12: 227-39.

Marcus, W. Andrew, Scott C. Ladd, Julie A. Stoughton, and Joseph W. Stock. 1995. Pebble counts and the role of user-dependent bias in documenting sediment size distributions. *Water Resources Research* 31, no. 10: 2625-31.

Petersen, James F. and Julie A. Tuason, eds. 1995a. *A geomorphic glimpse of central Texas and the Borderlands: Images and encounters*. Chapter 2: The southern Hill Country Region of Texas by Richard C. Jones. San Antonio, TX: Pathways in Geographic Resource Publications.

________. 1995b. *A geomorphic glimpse of central Texas and the Borderlands: Images and encounters*. Chapter 3: Along the edge of the Hill Country: The Texas Spring Line by James F. Petersen. San Antonio, TX: Pathways in Geographic Resource Publications.

Phillips, Jeff V. and Todd I. Ingersoll. 1997. Comparison of verified roughness coefficients for gravel-bed streams in central Arizona with other areas of the western United States. In *Floodplain management in a multi-faceted world: Proceedings of the twenty-first annual conference of the Association of State Floodplain Managers held in Little Rock, Arkansas 28 April-2 May 1997,* 154-58. Washington, DC: U. S. Geological Survey.

Richards, Keith S. 1982. *Rivers: Forms and processes in alluvial channels.* New York, NY: Methuen and Company.

Robison, E. George and Robert L. Beschta. 1989. Estimating stream cross-sectional area from wetted width and thalweg depth. *Physical Geography* 10, no. 2: 190-98.

Singer, Michael J. and Donald N. Munns. 1991. *Soils: An introduction.* New York, NY: Macmillan Publishing Company.

Slade, Raymond M., Jr., William H. Asquith, and Gary D. Tasker. 1995. *Multiple-regression equations to estimate peak flow frequency for streams in Hays County, Texas.* U. S. Geological Survey – Water-Resources Investigations Report 95-4019. Austin, TX: U. S. Geological Survey.

Swanson, Eric R. 1995. *Geo-Texas: A guide to the earth sciences*. College Station, TX: Texas A&M University Press.

Texas Parks and Wildlife Department. 2002. *Natural regions of Texas- major regions* [on-line]. Austin, TX: Texas Parks and Wildlife Department; available from http://www.tpwd.state.tx.us/gis/download.htm#maps; Internet. Accessed on 10 October 2002.

Tinkler, Keith J. 1997. Critical flow in rockbed streams with estimated values for Manning's *n*. *Geomorphology* 20: 147-64.

United States Geological Survey. 2002. *NWISWeb Data for Texas* [on-line]. Washington, DC: U. S. Geological Survey; available from http://waterdata.usgs.gov/tx/nwis/nwis; Internet. Accessed on 8 September 2002.

Wahl, Kenneth L., Wilbert O. Thomas, and Robert M. Hirsch. 1995. *Stream-gaging program of the U. S. Geological Survey*. U. S. Geological Survey Circular 1123. Reston, VA: U. S. Geological Survey.

Wolman, M. Gordon. 1954. A method of sampling coarse river-bed material. *Transactions of the American Geophysical Union* 35: 951-56.

VITA

Mindy Marie Conyers was born in Dallas, Texas, on March 22, 1977, the daughter of Jim and Sharon Conyers. After completing her work at Marcus High School in Flower Mound, Texas, in 1995, she entered Texas A&M University in College Station, Texas. She received the degree of Bachelor of Science from the University of North Texas in Geography in May of 2001. During her last two years of college she held a job as a Research Scientist at the Lewisville Aquatic Ecosystem Research Facility. In August 2001, Mindy entered Graduate School for a Master of Applied Geography at Southwest Texas State University in San Marcos, Texas. Throughout her graduate work, she was employed as a Graduate Assistant teaching Geographic Information Science labs for the SWT Geography Department.

Permanent Address: 6664 Orchard Drive
Flower Mound, Texas 75022

Mindy Marie Conyers typed this thesis.